Submillimeter-Wave Measurements and Analysis of the Ground and $\nu_2 = 1$ States of Water

Pin Chen[1], J. C. Pearson[2], Shuji Matsuura[3], Geoffrey A. Blake[3] and Herbert M. Pickett[2]

Received ; Accepted

[1] *Time and Frequency Division, National Institute of Standards and Technology, Mail Stop 847.10, 325 Broadway, Boulder, CO 80303*

[2] *Jet Propulsion Laboratory, California Institute of Technology, Mail Stop 183-301, 4800 Oak Grove Dr., Pasadena, CA 91109*

[3] *Division of Geological & Planetary Sciences, California Institute of Technology, Mail Stop 150-21, Pasadena, CA 91125*

ABSTRACT

In order to facilitate further studies of water in the interstellar medium, the envelopes of late type stars, jets, and shocked regions, the frequencies of 17 newly measured $H_2{}^{16}O$ transitions between 0.841 and 1.575 THz are reported. A complete update of the available water line frequencies and a detailed calculation of unmeasured rotational transitions and transition intensities as a function of temperature are presented for the ground and $\nu_2 = 1$ state levels below 3000 cm^{-1} of excitation energy. The new THz transitions were measured with a recently developed laser difference frequency spectrometer. Six of these transitions arise from the $\nu_2 = 1$ state and the other eleven are in the ground state; all have lower state energies from 700 to 1750 cm^{-1} and should be accessible to SOFIA through the atmosphere. The transitions near 0.850 THz are accessible from the ground with existing receivers. Observations of the newly measured $\nu_2 = 1$ state transitions, which include the $1_{1,1} - 0_{0,0}$ fundamental at 1.2057 THz and five other very low J transitions, should provide valuable insights into role played by the $\nu_2 = 1$ state in the cooling dynamics of jets, shocks, masers, and strongly infrared pumped regions. The line list is presented to assist in the planning of observational campaigns with FIRST and other proposed space missions where a full suite of water observations can be carried out.

Subject Headings: interstellar molecules - laboratory spectra - line identification - molecular process

1. INTRODUCTION

Among the miriad compounds now detected in the interstellar medium, water retains a special significance. From the atmospheres of late type stars or brown dwarfs to dense molecular clouds and the young stars they give birth to, water plays a critical role in the chemical and physical evolution of galaxies such as our own. Its strong dipole moment allows water vapor to contribute substantially to the cooling of interstellar gas over an extraordinary span of densities and temperatures, while its hydrogen bonding capabilities give it "universal solvent" properties, and allow it to exist in a liquid or solid state over a wide range of physical conditions. As such, water ice is the dominant component of volatile grain mantles in dense molecular clouds and planetesimals the outer regions of the solar system, while the life as we know it would be restricted to the so-called habitable zones around stars in which terrestrial planets can maintain liquid water on their surfaces over geological timescales (Kasting, Whitmire & Reynolds 1993).

Observation of extraterrestrial water vapor has always posed a major experimental challenge, however, due to it's presence in the earth's atmosphere. Indeed, water vapor provides the major source of atmospheric opacity from the millimeter-wave to far-infrared spectral region, and the need for low concentrations of atmospheric water is the primary selection criteria for the Atacama Large Millimeter Array (ALMA) and South Pole submillimeter sites (Radford & Holdaway 1998; Matsuo, Sakamoto & Matushima 1998). Despite the low precipitable water columns at these sites, there are still large regions of completely inaccessible frequencies due to atmospheric absorption. For observations from the Stratospheric Observatory For Infrared Astronomy (SOFIA), the problem is less severe due to the increased altitude; however, direct studies of the strongest transitions are still precluded by the atmosphere. This problem is particularly acute for the low lying ground state transitions now known to dominate the interstellar spectrum.

In spite of the observational difficulties, a number of water transitions, both from the parent isotopomer and from isotopically substituted species such as $H_2{}^{18}O$ and HDO, have been observed from the ground and the Kuiper Airborne Observatory (KAO). More recently, a large number of water transitions have been observed both in emission and absorption by the spectroscopic instruments onboard the Infrared Space Observatory (ISO) (e.g. Neufeld et al. 1996 and Liu et al. 1996). Two small observatories, NASA's Submillimeter Wave Astronomy Satellite (SWAS) and the Swedish Space Corporation's ODIN, are beginning

service with the primary mission goal being observations of the 557 GHz water fundamental (Melnick 1993, Melnick et al. 1996). On longer timescales, the Far-InfraRed Space Telescope (FIRST) mission offers the potential for detailed studies of large numbers of water lines, including the majority of those presented here, free of the usual atmospheric restrictions.

The prevalence of water in the atmosphere and the extensive studies undertaken to examine its effect on the transmission of electromagnetic communication signals notwithstanding, prediction of water transitions with the kind of accuracy required for heterodyne observations remains an elusive goal. A number of authors have attempted a wide variety of analysis techniques with limited success. Unfortunately, none of these methods have enabled the prediction of previously unobserved transitions to microwave precision. Infrared transitions can now be accurately predicted to very high J and K_a values, however, and there is considerable hope that additional high resolution data, especially in the $\nu_2 = 1$ state, will facilitate the same for the submillimeter-wave transitions. The current state-of-the-art in the calculation of water frequencies is to use a potential energy surface based on ab initio calculations (Partridge & Schwenke 1997). Several different methods of generating ab initio line lists have been developed (Viti, Tennyson & Polyansky 1997), and they have proven useful in assignment of the sunspot spectrum (Tennyson & Polyansky 1998, Polyansky et al. 1997a, Polyansky et al. 1997b). Under favorable conditions, the ab initio accuracy appears to be better than 0.01 cm^{-1}. This translates to errors of several hundred MHz in the pure rotational line frequencies, which is insufficient for heterodyne astronomy requirements. As a result, it is still necessary to utilize fits to observed data for an accurate determination of the water vapor pure rotational spectrum.

Two distinct methods for fitting experimental water spectra have been proposed and demonstrated in the literature: 1) effective approaches to the rotational Hamiltonian, such as Pade series (Burenin et al. 1983, Burenin & Tyuterev 1984), Borel approximates (Polyansky 1985, Belov et al. 1987), and generating functions (Tyuterev 1992, Starikov, Tashkun, & Tyuterev 1992; Mikhailenko et al. 1997); and 2) a potential function that describes one or more vibrational degrees of freedom (usually the bend) is combined with an effective Hamiltonian that addresses the remaining degrees of freedom (Jensen 1989; Coudert 1992, 1994, 1997). The best results will most likely emerge from the application of the second method using a version of the Partridge & Schwenke (1997) potential surface, empirically modified to reproduce the highest observed

levels (e.g. Csaszar et al. 1998), and an effective Hamiltonian fit to the experimental data to secure the extra precision needed. Unfortunately, calculations of this type have not yet managed to achieve the accuracy needed for predictions of unobserved transitions with heterodyne resolution (Coudert 1997). Some of the disparity is due to the relatively small number of very high resolution measurements, especially in the $\nu_2 = 1$ state. Over the last few years a number of high resolution far-infrared and infrared studies have been carried out, greatly improving the quality of the available water line data. In this paper we have re-analyzed the ground and $\nu_2 = 1$ state water spectra with a non-power series effective Hamiltonian. This approach has reproduced the data to within a factor of two of the experimental precisions and pointed out a number of potential problems with the existing data set.

The other difficult problem in water spectroscopy is the accurate prediction of relative and absolute line intensities. The current wisdom is to use a power series expansion of the dipole moment tensor (Suhm & Watts 1991; Shostak, Ebenstein, & Muenter 1991; Shostak & Muenter 1991; Kjaergaard et al. 1994; Kjaergaard & Henry 1994; Mengel & Jensen 1995; Coudert 1997; Toth 1998). The dipole expansion presented in the latter of these references is in good agreement with the observed data for $J < 15$. However, the dipole expansion has yet to be applied to highly excited levels, and is therefore likely to suffer from the same problems as the energy level calculations. As a result, little is known about how well these dipole expansions will predict intensities at larger rotational quantum numbers. Calculation of the intensities of the low lying rotational transitions in the microwave region should be good to better than 5% with the two most recent dipole expansions. The greatest deviations from the predicted intensities are expected in the higher J transitions with $\Delta K_a > 3$. In the intensity calculations presented here, the measured dipole moment parameters of Shostak, Ebenstein, & Muenter (1991) and Shostak & Muenter (1991) have been used along with the planarity conditions as described by Watson (1971) in a computational method developed by Camy-Peyret et al. (1985).

The precision measurements of a number of additional $H_2{}^{16}O$ transitions are reported to facilitate their astronomical observation and to support efforts in developing better molecular models for the calculation of the energy levels and transition intensities in water. The measurements reported in this paper are the first to be carried out with a new spectrometer system that uses optical-heterodyne conversion to generate THz

radiation. This spectrometer should facilitate the precision measurement of a variety of species in the 0.3 to 3.0 THz region in support of FIRST and SOFIA. The transition list reported in Pearson et al. (1991) is also updated to include the large number of high accuracy measurements made over the last few years. The calculations presented represent the state-of-the-art, and should be sufficient for all far-infrared astronomical observations except those of the hottest and most highly shocked regions, and should prove useful in planning the THz heterodyne receiver science programs for FIRST and SOFIA.

2. EXPERIMENTAL

The experimental measurements were carried out with a three-diode-laser, difference-frequency spectrometer, an outline of which is presented in Figure 1. Laser #1 is locked, using a Pound-Drever-Hall approach (Pound 1946, Drever et al. 1983), to a temperature stabilized ultra-low expansion (ULE) Fabry-Perot etalon (whose thermal expansion coefficient is of order $\sim 2 \times 10^{-10}$ /C). Laser #2 is Pound-Drever-Hall locked to the same etalon a large integer number of free spectral ranges away, and laser #3 is offset locked with a phase locked loop to laser #2. This phase locked offset frequency is controlled by a tunable 2–6 GHz microwave synthesizer. Beating simultaneously amplified signals from lasers #1 and #3 in a low-temperature-grown GaAs photomixer coupled to a planar submillimeter antenna (Verghese, McIntosh & Brown 1997) generates the THz difference frequency. The free spectral range of the etalon was calibrated to 5 parts in 10^8 by measuring all CO pure rotational lines from 230 – 1611 GHz. A detailed description of this laser system and the calibration method can be found elsewhere (Matsuura et al. 1999). The measurement accuracy is currently limited by the uncertainty in the free spectral range, a small drifting DC residual in the lock loops, and the accuracy of determining the center of the transition. The line width of the spectrometer is $\gtrsim 1$ MHz (the THz frequency stability is considerably better), enabling doppler-limited resolution to be obtained. As a result, the expected measurement accuracy is calculated to be of order 250 kHz for a 1σ measurement. The $4_{2,2} - 3_{3,1}$ ground state transition was re-measured as a verification of the spectrometer calibration. Our observed value of 916171.270 MHz agrees within the expected 250 kHz experimental error with both the 916171.582(150) harmonic generation value reported by Helminger et al. (1983) and the 916171.405(13) laser sideband value reported by Matsushima et al. (1995).

Initial predictions were made from energy levels calculated by Toth (1998) and from previous uncalibrated

backward wave oscillator measurements (Belov 1996). The water sample was reagent grade and required no further processing. Measurements were made in a single pass 1.6 meter long cell under continuous flow conditions at pressures of approximately 100 mTorr. A 1.8 Kelvin composite-silicon bolometer was used to detect the tunable THz radiation. The source was chopped at 100 Hz and 200 Hz lock-in detection was used to record the line profiles. Forward and backward scans were averaged to eliminate the lock-in time constant drift, while the line centers were determined by either fitting a parabola to the peak of the observed transition or by taking the midpoint between the half-intensity frequencies. Signal-to-noise ratios for the observed lines ranged from 10 to $\gtrsim 500$. Several measurements of each line were made for consistency.

All the measured transitions fell within the quoted experimental errors of Toth (1998). The agreement with the uncalibrated measurements of Belov (1996) is better than one MHz in all cases, suggesting that the previous data are accurate to at least this level. Table 1 presents the results of this study along with the expected positions from Toth (1998) and the uncalibrated measurements of Belov (1996). Clearly, all the reported transitions agree extremely well with the energy levels of Toth (1998). This was expected since a series of combination difference calculations with our measurements and the transitions of Matsushima et al. (1995) used in the Toth (1998) compilation closed to within experimental accuracy. Table 2 is a set of measurements from Pearson (1995) compared to the energy levels from Toth (1998) for the $\nu_2 = 1$ state and from Toth (1999a) for the $\nu_2 = 2$ or (020), $\nu_1 = 1$ or (100) and $\nu_3 = 1$ or (001) states. Once again, all the measurements – with the exception of the 14 MHz deviation of the (020) $4_{2,2} - 3_{3,1}$ transition – agree to within the experimental uncertainty. The reason for the large deviation of the $4_{2,2} - 3_{3,1}$ transition is unclear and a cause for some concern. The 17 transitions measured as a part of this work, the two reported from Belov (1996), and the nine from Pearson (1995) have not appeared in the widely published literature. Table 3 presents a list of all the reported microwave accuracy measurements for $H_2{}^{16}O$ below 4 THz, and also includes the observed minus calculated frequency differences and the lower state energy of the fit. The lower state energy from Toth (1998) is given as well.

3. ANALYSIS

The experimental data used in the analysis included the following:

1) The microwave transitions reported in Table 3. The measurements from Matsushima et al. (1995) were

assumed to have an experimental accuracy of 150kHz. This was derived from a series of arithmetic calculation of residuals around closed loops of four transitions and is consistent with 5% of the FWHM of a water line profile at these frequencies.

2) The term values from Toth (1998) and Polyansky et al. (1997b) through $J = 19$ and 18 in the ground and $\nu_2 - 1$ states, respectively.

3) Infrared rotational transitions, including measurements unique to Kauppinen et al. (1978), Johns (1985), Paso and Horneman (1995) and Toth (1999b).

4) Infrared ν_2 band transitions from Toth (1999b).

In the event of repeated measurements, the value used in the fit was the microwave frequency or the most recent infrared measurement. The model used was a non-power series effective Hamiltonian related to both the Pade Series and the generating functions discussed in the Introduction. The details of the calculation and the model will be presented in an appropriate forum elsewhere. The reduced RMS of the fit [reduced RMS = absolute RMS (MHz)/experimental error (MHz)] was 1.98 if all the data were forced into the fit and 1.61 if the fit was allowed to reject 13 out of 3992 lines and energy levels. Reduced RMS values of 1.78 and 1.41 were achieved with a slightly reduced data set, with the same exact same 13 lines being rejected in the reduced analysis. It is interesting to note that the majority of the rejected transitions (a total of eight) involved the $15_{6,10}$ level of the $\nu_2 = 1$ state and that the deviations were all of the same direction and magnitude to much better than the experimental accuracy, suggesting either a fitting artifact or a local perturbation. Due to the form of these deviations the results presented here are from a fit where all the transitions were forced into the calculation. The intensity calculations used a Watson A-like constant set and a fixed S-like d_2 constant determined from the planarity conditions. The fixed d_2 constant can be removed, however, and quality of the fit is largely unchanged. Higher order contributions to the dipole were calculated using the procedure presented by Camy-Peyret et al. (1985). The intensities generated by these calculations were compared to those of Toth (1998) at 296 K and were found to be in reasonable agreement for all transition changing K_a by 1 or 3. Since the dipole expansion used does not include the planarity conditions for the P^6 and higher order terms, the transitions changing K_a by more than three will not be correct and large deviations do exist between the measured intensities and the calculated values. It should

be noted that there are none of these transition in the data presented.

Table 4 presents a listing of all of the water rotational transitions below 4 THz and 3000 cm^{-1} of total energy. It includes the calculated frequency, the calculated uncertainty in the line position, the ${}^{m}S_{ba}\mu^2$ values, the lower and upper state energies state energies, and the factors $[e^{-E''/kT} - e^{-E'/kT}]$ at 50, 200, 800 and 1500 K. The error in the calculation frequency assumes that the reduced RMS of the fit is one, since it is nearly 2 the error quoted is approximately 0.5σ. The partition function determined as a function of temperature by a sum over all states up to J=23 is listed in Table 5. It does not include contributions for higher J states or the next higher set of vibrational levels. At temperatures above 500 K there will begin to be a significant contribution by these levels, by 1500 K they must be included if accurate values are to be determined. To first order the partition function can be corrected by separating the vibrational part of the partition function and calculating a correction factor. A first order correction for the next 3 vibrational states (020), (100), (001) (030), (110) and (011), which all have a number of levels below the rotational energy considered in the rotational part of the calculation, is also given on Table 5. Multiplication of the rotational partition function given by the correction factor will give a better estimate of the true partition function at high temperatures, but it will not take care of contributions from higher rotational states. A full calculation including the ν_3 band will be placed in the JPL spectral line catalog at **http://spec.jpl.nasa.gov**. A graphical summary of the local thermodynamic equilibrium, or LTE, line intensities at various temperatures for a fixed column density is presented in Figure 2. By 1500 K the majority of the lines are within a factor of a few in intensity and the strongest lines are from states that are relatively weak at room temperature and almost unpopulated at typical dense molecular cloud temperatures. It should also be noted that there is a two order of magnitude reduction in the intensity of the strongest line.

The LTE line intensities and other parameters can be calculated from the data given on Table 4 and Table 5 using the following equations:

$$I_{ba}(T) = (8\pi^3/3hc)\nu_{ba}{}^{x}S_{ba}\mu^2[e^{-E''/kT} - e^{-E'/kT}]/Q_{rs} \tag{1}$$

$$I_{ba}(T) = I_{ba}(T_0)[Q_{rs}(T_0)/Q_{rs}(T)][(e^{-E''/kT} - e^{-E'/kT})/(e^{-E''/kT_0} - e^{-E'/kT_0})] \tag{2}$$

$$I_{ba}(T) = I_{ba}(T_0)(T_0/T)^{5/2}e^{-(1/T-1/T_0)E''/k} \tag{3}$$

In equation (1), ν_{ab} is the line frequency, $^{*}S_{ab}$ is the line strength including the degeneracy factors, μ is the dipole moment along the b axis, E'' and E' are the lower and upper state energies, respectively, and Q_{ns} is the rotation-spin partition function.

The line frequency and LTE intensity data alone are, of course, insufficient to explain the excitation of water in the interstellar medium – especially the 1594 cm^{-1} $\nu_2 = 1$ state of water – for which a combination of collisions and radiative processes must be considered. Indeed, the $1_{1,0} - 1_{0,1}$ $\nu_2 = 1$ fundamental at 658 GHz is known to mase strongly in a number of regions (Menten & Young 1995), and a number of other low lying $\nu_2 = 1$ transitions, such as the $1_{1,1} - 0_{0,0}$ line reported here, should be bright masers through the same pumping mechanism. Even in the ground state, a more realistic assessment of the source structure leads to water transitions appearing both in emission and absorption (Zmuidzinas 1996). A detailed understanding of how water is excited, including maser action, requires knowledge of both the radiation and density environment along with the strengths of the ν_2 band transitions. The line strengths for the ν_2 band have been measured in some detail for the atmospheric community and can be found in Toth (1998). The Toth (1998) line strengths are given in cm^{-2}/atm at 296 K can be converted to the nm^{2}MHz units used in the JPL catalog by multiplying by a factor of 247938.0 (Avagadro's number divided by a mole volume in cm^3 at 296 K $\times$ 10^{-14}). The factor of 10^{-14} converts the nm^{2}MHz JPL catalog unit into cm^{2}MHz units, which are often more natural for calculations. Division by a factor of $2.99792458 \times 10^{18}$ converts the catalog units into the commonly given infrared units of cm^{-1}/(molecule/cm^2)

CONCLUSIONS

Recently, ISO has observed a large number of water emission lines in a wide variety of astronomical sources. As a result, the pivotal role water plays in cooling oxygen rich molecular gas is now well established. If the high temperatures inferred from CO observations of many of these regions are proven to apply to water as well, the number of states considered in the current models are grossly inadequate, and most of the details of the excitation dynamics have been blended by a near continuum of water emission lines. At such high temperatures, very high spectral resolution is required to deconvolute the true continuum from the water lines. Heterodyne observation of lines such as those presented in this paper would facilitate direct observations of hot sources and measurements of the rotational temperatures therein. An accurate

temperature measurement will define the severity of the prediction problem for water. If the temperature really is much above 300 K, future missions such as FIRST and SOFIA will observe many strong water lines, including a large number above the energies considered here. Analyses of these observations will require extended calculations that include a good many more quantum states than those considered here, especially levels in the $\nu_2 = 2$, $\nu_1 = 1$ and $\nu_3 = 1$ states, and a great deal more laboratory work. At a minimum, the data presented here should be sufficient for planning observations of all but the most highly shocked and hottest regions.

Acknowledgements

The portions of the work performed at Jet Propulsion Laboratory were done under contract with the National Aeronautics and Space Administration (NASA). G.A. Blake acknowledges the support of NASA and the National Science Foundation. We thank Dr. Simon Verghese of MIT Lincoln Laboratories for supplying the photomixers used in this study. J C. Pearson thanks Dr. Robert A. Toth for making available his latest water measurements prior to publication and for useful discussions concerning their analysis.

Belov, S.P., Kozin, I.N., Polyansky, O., Yu. M., Tret'yakov, M. & Zubov, N. 1987, J. Mol. Spectrosc., 126, 113.

Belov, S.P. 1996, private communication.

Burenin, A., Fevral'skikh, M., Klaryakin, E., Polyansky, O.L., & Shapin S. 1983, J. Mol. Spectrosc., 100, 182.

Burenin, A.V. & Tyuterev, V.G. 1984, J. Mol. Spectrosc., 108, 153.

Camy-Peyret, C. et al. 1985, J. Mol. Spectrosc., 113, 208.

Coudert, L.H. 1994, J. Mol. Spectrosc., 165, 406.

Coudert, L.H. 1992, J. Mol. Spectrosc., 154, 427.

Coudert, L.H. 1997, J. Mol. Spectrosc., 181, 246.

Csaszar, A.G., Kain, J.S., Polyansky, O.L., Zobov, N.F. &. Tennyson, J. 1998, Chem. Phys. Lett., 293, 317.

Drever, R.W.P., Hall, J.L., Kowalski, F.V., Hough, J., Ford, G.M. Munley, A.J. & Ward, H. 1983, Appl. Phys. B, 31, 97.

Helminger, P., Messer, J.K., De Lucia, F.C. 1983, Appl. Phys. Lett., 42, 309.

Jensen, P. 1989, J. Mol. Spectrosc., 133, 438.

Johns, J.W.C. 1985, J. Opt. Soc. Am. B, 2, 1340.

Kasting, J.F., Whitmore, D.P. & Reynolds, R.T. 1993, Icarus, 101, 108.

Kauppinen, J., Karkkainen, T., &Kyro, E. 1978, J. Mol. Spectrosc., 71, 15.

Kjaergaard, H.G., Henry, B.R., Wei, H., Lefebvre, S., Carrington , T., Jr., Mortensen, O.S. & Sage, M.L. 1994, J. Chem. Phys., 100, 6228.

Kjaergaard, H.G. & Henry, B.J. 1994, Mol. Phys., 83, 1099.

Liu, X.W. et al., 1996, A&A, 315, L257.

Matsuo, H., Sakamoto, A., & Matsushita, S. 1998, SPIE, Vol. 3357, 626.

Matsushima, F., Odashima, H., Iwasaki, T., Tsunekawa, S., Takagi, K. 1995, J. Mol. Struct., 352-353, 371.

Matsuura, S., Chen, P., Blake, G.A., Pearson, J.C., & Pickett, H.M. 1999, IEEE MTT, in press

Melnick, G.J. 1993, Adv. Space Res., 13, 535.

Melnick, G.J. et al. 1996, Adv. Space Res., 18, 163.

Mengel, M. & Jensen, P. 1995, J. Mol. Spectrosc., 169, 73.

Menten, K. and Young, K., 1995, ApJ, 450, L67.

Mikhailenko, S.N., Tyuterev, V.G., Koppler, K.A., Winnowisser, B.P., Winnowisser, M., Mollau, G., Klee, S. & Rao, K.N. 1997, J. Mol. Spectrosc., 184, 330.

Neufeld, D.A., Chen, W., Melnick, G.J., de Graauw, T., Feuchtgruber, H., Haser, L., Lutz, D. & Harwit, M. 1996, A&A, 315, L237.

Partridge, H. & Schwenke, D.W. 1997, J. Chem. Phys., 106, 4618.

Paso, R. & Horneman, V.M. 1995, J. Opt. Soc. Am. B, 12, 1813.

Pearson, J.C. 1991, ApJ, 379, L41.

Pearson, J.C. 1995, Ph.D. Thesis, Duke University.

Polyansky, O.L. 1985, J. Mol. Spectrosc., 112, 79.

Polyansky, O.L., Zobov, N.F., Viti, S., Tennyson, J., Bernath, P.F., & Wallace, L. 1997a, Science, 277, 346.

Polyansky, O.L., Zobov, N.F., Viti, S., Tennyson, J., Bernath, P.F., & Wallace, L. 1997b, J. Mol. Spectrosc., 186, 422.

Pound, R.V. 1946, Rev. Sci. Instrum., 17, 490.

Radford, S.J.E. & Holdaway, M.A. 1998, SPIE, Vol. 3357, 486.

Shostak, S.L., Ebenstein, W.L. & Muenter, J.S. 1991, J. Chem. Phys., 94, 5875.

Shostak, S.L. & Muenter, J.S. 1991, J. Chem. Phys., 94, 5883.

Starikov, V.I., Taskun, S.A., & Tyutrev, V.G. 1992, J. Mol. Spectrosc., 151, 130.

Suhm, M.A. & Watts, R.O. 1991, Mol. Phys., 73, 463.

Tennyson, J. & Polyansky, O.L. 1998, Cont. Phys., 39, 283.

Toth, R.A. 1998, J. Mol. Spectrosc., 190, 379.

Toth, R.A. 1999a, J. Mol. Spectrosc., 194, 28.

Toth, R.A. 1999b, private communication.

Tyuterev, V.G. 1992, J. Mol. Spectrosc., 151, 97.

Verghese, S., McIntosh, K.A., & Brown, E.R. 1997, Appl. Phys. Lett., 71, 2743.

Viti, S., Tennyson, J., & Polyansky, O.L. 1997, MNRAS, 287, 79.

Watson, J.K.G. 1971, J. Mol. Spectrosc., 40, 536.

Zmuidzinas, J. 1996. in *Proc. 30th ESLAB Symp.*, ESA SP-388, 151.

Table 1. Water Transitions Measured with the THz Photomixer Spectrometer

Transition	Observed Frequency (MHz)	Toth (1998) (MHz)	Belov (1996) (MHz)
$10_{5,6} \rightarrow 11_{2,9}$ (000)	841051.162(250)	841050.35(1.50)	841050.56(1.00)
$10_{8,3} \rightarrow 9_{9,0}$ (000)	...	863842.67(2.70)	863838.93(1.00)
$9_{2,8} \rightarrow 8_{3,5}$ (000)	906206.118(250)	906205.78(0.39)	
$7_{2,5} \rightarrow 8_{1,8}$ (000)	1146621.161(250)	1146621.04(0.39)	
$8_{5,4} \rightarrow 7_{6,1}$ (000)	1168358.526(250)	1168358.57(0.48)	
$7_{4,4} \rightarrow 6_{5,1}$ (000)	1172525.835(250)	1172525.90(0.48)	
$8_{5,3} \rightarrow 7_{6,2}$ (000)	1190828.878(250)	1190828.80(0.48)	
$9_{6,4} \rightarrow 8_{7,1}$ (000)	1215801.676(250)	1215801.87(0.84)	
$9_{6,3} \rightarrow 8_{7,2}$ (000)	1219943.736(250)	1219943.68(0.90)	
$8_{4,5} \rightarrow 9_{1,8}$ (000)	1307963.124(250)	1307963.17(0.48)	
$7_{4,4} \rightarrow 8_{1,7}$ (000)	1344676.488(250)	1344676.29(0.48)	
$6_{4,3} \rightarrow 7_{1,6}$ (000)	1574232.073(250)	1574232.14(0.39)	
$2_{1,1} \rightarrow 2_{0,2}$ (010)	859965.649(250)	859966.36(0.90)	
$2_{0,2} \rightarrow 1_{1,1}$ (010)	899302.171(250)	899301.23(1.80)	899301.92(1.00)
$3_{1,2} \rightarrow 2_{2,1}$ (010)	902609.436(250)	902610.64(2.70)	902609.31(1.00)
$6_{2,5} \rightarrow 5_{3,2}$ (010)	...	923113.74(1.80)	923113.19(1.00)
$1_{1,1} \rightarrow 0_{0,0}$ (010)	1205788.640(250)	1205788.95(2.70)	
$3_{1,2} \rightarrow 3_{0,3}$ (010)	1214662.064(250)	1214663.11(2.40)	
$2_{2,0} \rightarrow 2_{1,1}$ (010)	1494057.154(250)	1494057.39(0.60)	

Table 2. Additional Water THz Measurements from Pearson (1995)

Transition	Observed Frequency (MHz)	Toth (1998) (MHz)
$8_{8,1} \rightarrow 9_{7,2}$ (010)	129811.529(100)	129812.23(2.70)
$8_{8,0} \rightarrow 9_{7,3}$ (010)	129889.509(100)	129889.28(3.00)
$4_{2,2} \rightarrow 3_{3,1}$ (020)	137048.521(100)	137062.41(2.70)
$6_{3,3} \rightarrow 5_{4,2}$ (020)	147521.501(100)	147521.57(2.40)
$3_{1,3} \rightarrow 2_{2,0}$ (020)	516229.985(150)	516230.02(3.00)
$6_{4,3} \rightarrow 5_{5,0}$ (100)	376549.519(150)	376549.52(1.80)
$5_{3,3} \rightarrow 4_{4,0}$ (100)	464345.834(150)	464345.84(3.60)
$3_{1,3} \rightarrow 2_{2,0}$ (001)	254039.880(150)	254039.33(1.50)
$4_{1,4} \rightarrow 3_{2,1}$ (001)	430012.786(150)	430012.11(1.80)

Table 3. The Microwave and THz Data Set Used in the Water Spectrum Fit

$J''K''_aK''_cV'' \rightarrow J'K'_aK'_cV'$	Frequency (MHz)	O-C (MHz)	Unc.(kHz)	Ref.
4 2 2 1 → 5 1 5 1	2159.980	-0.059	300	A
4 2 3 1 → 3 3 0 1	12008.800	0.002	30	A
6 1 6 0 → 5 2 3 0	22235.080	-0.037	20	A
5 3 2 1 → 4 4 1 1	26834.270	0.029	30	A
4 1 4 1 → 3 2 1 1	67803.960	-0.030	40	A
4 4 0 1 → 5 3 3 1	96261.160	0.309	100	A
2 2 0 1 → 3 1 3 1	119995.940	-0.195	100	A
8 8 1 1 → 9 7 2 1	129811.529	0.157	150	B
8 8 0 1 → 9 7 3 1	129889.509	-0.010	150	B
14 6 9 0 → 15 3 12 0	139614.293	1.320	150	A
15 6 10 0 → 16 3 13 0	177317.068	-0.947	150	A
3 1 3 0 → 2 2 0 0	183310.117	0.087	50	A
5 5 1 1 → 6 4 2 1	209118.370	-0.012	150	A
5 5 0 1 → 6 4 3 1	232686.700	0.145	150	A
14 4 10 0 → 15 3 13 0	247440.096	-0.051	150	A
13 6 8 0 → 14 3 11 0	259951.444	-1.169	150	A
7 7 1 1 → 8 6 2 1	262897.748	0.120	150	A
7 7 0 1 → 8 6 3 1	263451.357	-0.169	150	A
6 6 1 1 → 7 5 2 1	293664.442	0.044	150	A
6 6 0 1 → 7 5 3 1	297439.107	-0.307	150	A
10 2 9 0 → 9 3 6 0	321225.640	-0.016	50	A
14 3 12 1 → 13 4 9 1	323554.019	0.293	150	A
5 1 5 0 → 4 2 2 0	325152.919	-0.016	50	A
5 2 3 1 → 6 1 6 1	336227.620	-0.311	150	A
16 6 11 0 → 17 3 14 0	339043.996	0.320	150	A
17 4 13 0 → 16 7 10 0	354808.877	0.051	150	A
4 1 4 0 → 3 2 1 0	380197.372	0.006	50	A
10 3 7 0 → 11 2 10 0	390134.508	-0.133	50	A
8 5 4 1 → 7 6 1 1	425689.190	-0.101	150	A
7 5 3 0 → 6 6 0 0	437346.667	0.016	50	A
9 6 4 1 → 8 7 1 1	438724.178	1.149	150	A
6 4 3 0 → 5 5 0 0	439150.812	-0.059	50	A
8 5 3 1 → 7 6 2 1	440736.910	-0.796	150	A
9 6 3 1 → 8 7 2 1	441238.866	-0.406	150	A
7 5 2 0 → 6 6 1 0	443018.295	-0.017	50	A
4 2 3 0 → 3 3 0 0	448001.075	-0.059	50	A
4 2 2 1 → 3 3 1 1	463170.460	-0.243	250	A
6 4 2 0 → 5 5 1 0	470888.947	-0.056	50	A
5 3 3 0 → 4 4 0 0	474689.127	-0.130	50	A
6 2 4 0 → 7 1 7 0	488491.133	0.061	50	A

Table 3—Continued

$J''K''_aK''_cV'' \rightarrow J'K'_aK'_cV'$	Frequency (MHz)	O-C (MHz)	Unc.(kHz)	Ref.
7 4 4 1 → 6 5 1 1	498502.590	0.241	150	A
8 6 3 0 → 7 7 0 0	503568.532	-0.305	100	A
8 6 2 0 → 7 7 1 0	504482.692	-0.307	100	A
14 3 12 0 → 13 4 9 0	530342.834	0.083	150	A
5 2 4 1 → 4 3 1 1	546690.600	-0.098	150	A
10 7 4 1 → 9 8 1 1	548474.403	-0.524	150	A
1 1 0 0 → 1 0 1 0	556936.002	0.014	50	A
12 6 7 0 → 13 3 10 0	571913.392	-0.729	150	A
7 4 3 1 → 6 5 2 1	578057.486	0.206	150	A
9 2 8 1 → 8 3 5 1	593708.497	-0.192	150	A
6 3 4 1 → 5 4 1 1	595079.800	-0.158	150	A
5 3 2 0 → 4 4 1 0	620700.807	-0.308	100	A
9 7 3 0 → 8 8 0 0	645766.010	-0.044	100	A
9 7 2 0 → 8 8 1 0	645905.620	0.056	100	A
1 1 0 1 → 1 0 1 1	658006.550	0.075	100	A
2 1 1 0 → 2 0 2 0	752033.227	0.095	100	A
10 5 6 0 → 11 2 9 0	841051.162	0.689	250	C
2 1 1 1 → 2 0 2 1	859965.649	0.228	250	C
10 8 3 0 → 9 9 0 0	863838.930	1.908	1000	D
2 0 2 1 → 1 1 1 1	899302.171	0.188	250	C
3 1 2 1 → 2 2 1 1	902609.436	0.078	250	C
9 2 8 0 → 8 3 5 0	906206.118	0.179	250	C
4 2 2 0 → 3 3 1 0	916171.582	0.073	100	A
6 2 5 1 → 5 3 2 1	923113.190	-0.374	1000	D
5 2 4 0 → 4 3 1 0	970315.022	-0.075	100	A
3 1 2 0 → 3 0 3 0	1097364.791	-0.114	150	E
1 1 1 0 → 0 0 0 0	1113342.964	0.047	150	E
7 2 5 0 → 8 1 8 0	1146621.161	-0.161	250	C
3 1 2 0 → 2 2 1 0	1153126.822	0.146	150	E
6 3 4 0 → 5 4 1 0	1158323.743	-0.149	150	E
3 2 1 0 → 3 1 2 0	1162911.593	-0.107	150	E
8 5 4 0 → 7 6 1 0	1168358.526	0.009	250	C
7 4 4 0 → 6 5 1 0	1172525.835	-0.024	250	C
8 5 3 0 → 7 6 2 0	1190828.878	-0.014	250	C
1 1 1 1 → 0 0 0 1	1205788.640	-0.663	250	C
4 2 2 0 → 4 1 3 0	1207638.714	0.002	150	E
3 1 2 1 → 3 0 3 1	1214662.064	0.295	250	C
9 6 4 0 → 8 7 1 0	1215801.676	-0.060	250	C
9 6 3 0 → 8 7 2 0	1219943.736	-0.638	250	C
2 2 0 0 → 2 1 1 0	1228788.772	-0.068	150	E

Table 3—Continued

$J''K''_aK''_cV'' \rightarrow J'K'_aK'_cV'$	Frequency (MHz)	O-C (MHz)	Unc.(kHz)	Ref.
7 4 3 0 → 6 5 2 0	1278265.946	0.023	150	E
8 2 7 0 → 7 3 4 0	1296411.033	-0.016	150	E
8 4 5 0 → 9 1 8 0	1307963.124	-0.163	250	C
6 2 5 0 → 5 3 2 0	1322064.803	0.020	150	E
7 4 4 0 → 8 1 7 0	1344676.488	0.312	250	C
5 2 3 0 → 5 1 4 0	1410618.074	0.087	150	E
7 2 6 0 → 6 3 3 0	1440781.544	-0.121	150	E
2 2 0 1 → 2 1 1 1	1494057.154	-0.332	250	C
6 3 3 0 → 5 4 2 0	1541966.785	-0.265	150	E
6 4 3 0 → 7 1 6 0	1574232.073	0.006	250	C
4 1 3 0 → 4 0 4 0	1602219.182	-0.160	150	E
2 2 1 0 → 2 1 2 0	1661007.637	-0.125	150	E
2 1 2 0 → 1 0 1 0	1669904.775	0.023	150	E
4 3 2 0 → 5 0 5 0	1713882.973	0.021	150	E
3 0 3 0 → 2 1 2 0	1716769.633	0.100	150	E
6 3 3 0 → 6 2 4 0	1762042.791	0.132	150	E
7 3 5 0 → 6 4 2 0	1766198.748	0.005	150	E
6 2 4 0 → 6 1 5 0	1794788.953	0.030	150	E
7 3 4 0 → 7 2 5 0	1797158.762	0.029	150	E
5 3 2 0 → 5 2 3 0	1867748.594	0.127	150	E
8 4 5 0 → 7 5 2 0	1884887.822	-0.091	150	E
5 2 3 0 → 4 3 2 0	1918485.324	-0.117	150	E
3 2 2 0 → 3 1 3 0	1919359.531	0.011	150	E
8 3 5 0 → 8 2 6 0	2015982.828	-0.019	150	E
4 3 1 0 → 4 2 2 0	2040476.810	0.051	150	E
4 1 3 0 → 3 2 2 0	2074432.305	-0.076	150	E
3 1 3 0 → 2 0 2 0	2164131.980	-0.021	150	E
3 3 0 0 → 3 2 1 0	2196345.756	-0.034	150	E
5 1 4 0 → 5 0 5 0	2221750.500	0.094	150	E
8 3 6 0 → 7 4 3 0	2244810.924	-0.130	150	E
4 2 3 0 → 4 1 4 0	2264149.650	0.092	150	E
9 4 5 0 → 9 3 6 0	2317882.160	0.056	150	E
7 2 5 0 → 7 1 6 0	2344250.335	-0.027	150	E
10 4 6 0 → 10 3 7 0	2347482.172	0.133	150	E
3 3 1 0 → 3 2 2 0	2365899.659	0.074	150	E
4 0 4 0 → 3 1 3 0	2391572.628	0.068	150	E
9 3 6 0 → 9 2 7 0	2428247.209	-0.115	150	E
8 4 4 0 → 8 3 5 0	2446843.245	-0.122	150	E
4 3 2 0 → 4 2 3 0	2462933.032	0.045	150	E
9 3 7 0 → 8 4 4 0	2531917.811	0.097	150	E

Table 3—Continued

$J''K''_aK''_cV'' \rightarrow J'K'_aK'_cV'$	Frequency (MHz)	O-C (MHz)	Unc.(kHz)	Ref.
7 3 4 0 → 6 4 3 0	2567177.132	0.104	150	E
11 4 7 0 → 11 3 8 0	2571762.630	0.113	150	E
10 3 8 0 → 9 4 5 0	2575004.634	0.216	150	E
5 3 3 0 → 5 2 4 0	2630959.520	0.146	150	E
4 1 4 0 → 3 0 3 0	2640473.836	-0.135	150	E
7 4 3 0 → 7 3 4 0	2664570.704	-0.080	150	E
5 2 4 0 → 5 1 5 0	2685638.969	0.048	150	E
2 2 1 0 → 1 1 0 0	2773976.588	0.062	150	E
12 5 7 0 → 12 4 8 0	2848996.260	0.468	150	E
6 3 4 0 → 6 2 5 0	2880025.369	0.075	150	E
6 1 5 0 → 6 0 6 0	2884278.940	0.055	150	E
6 4 2 0 → 6 3 3 0	2884941.052	0.012	150	E
6 2 4 0 → 5 3 3 0	2962111.094	-0.098	150	E
2 2 0 0 → 1 1 1 0	2968748.654	0.134	150	E
5 1 4 0 → 4 2 3 0	2970800.244	-0.196	150	E
11 5 6 0 → 11 4 7 0	2997539.160	0.364	150	E
8 2 6 0 → 8 1 7 0	2998565.722	0.106	150	E
10 3 7 0 → 10 2 8 0	3003347.566	-0.031	150	E
5 0 5 0 → 4 1 4 0	3013199.566	-0.027	150	E
5 4 1 0 → 5 3 2 0	3043766.149	-0.036	150	E
10 4 7 0 → 9 5 4 0	3118998.512	-0.730	150	E
4 4 0 0 → 4 3 1 0	3126585.070	-0.144	150	E
5 1 5 0 → 4 0 4 0	3135010.951	-0.038	150	E
9 4 5 0 → 8 5 4 0	3149876.898	-0.069	150	E
4 4 1 0 → 4 3 2 0	3165532.734	-0.059	150	E
6 2 5 0 → 6 1 6 0	3167578.237	0.103	150	E
5 4 2 0 → 5 3 3 0	3182186.848	0.047	150	E
7 3 5 0 → 7 2 6 0	3210358.196	0.078	150	E
6 4 3 0 → 6 3 4 0	3230146.525	0.107	150	E
10 5 5 0 → 10 4 6 0	3245323.573	0.269	150	E
11 5 7 0 → 10 6 4 0	3307402.532	-0.528	150	E
7 4 4 0 → 7 3 5 0	3329185.239	0.037	150	E
3 2 2 0 → 2 1 1 0	3331458.376	-0.014	150	E
8 4 5 0 → 8 3 6 0	3495358.110	-0.095	150	E
9 5 4 0 → 9 4 5 0	3509431.278	-0.005	150	E
7 1 6 0 → 7 0 7 0	3536666.807	0.096	150	E
6 0 6 0 → 5 1 5 0	3599641.708	0.029	150	E
8 3 6 0 → 8 2 7 0	3612970.623	-0.165	150	E
6 1 6 0 → 5 0 5 0	3654603.282	-0.228	150	E
8 3 5 0 → 7 4 4 0	3669872.251	-0.036	150	E

Table 3—Continued

$J''K''_aK''_cV'' \rightarrow J'K'_aK'_cV'$	Frequency (MHz)	O-C (MHz)	Unc. (kHz)	Ref.
11 3 8 0 → 11 2 9 0	3674226.995	-0.175	150	E
9 2 7 0 → 9 1 8 0	3682708.105	0.046	150	E
7 2 6 0 → 7 1 7 0	3691315.309	-0.088	150	E
11 5 6 0 → 10 6 5 0	3718095.940	0.223	150	E
8 5 3 0 → 8 4 4 0	3721502.796	0.058	150	E
9 4 6 0 → 9 3 7 0	3737021.532	0.030	150	E
6 1 5 0 → 5 2 4 0	3798281.638	-0.005	150	E
4 2 3 0 → 3 1 2 0	3807258.412	-0.213	150	E
7 5 2 0 → 7 4 3 0	3855281.595	0.250	150	E
6 5 1 0 → 6 4 2 0	3922858.136	0.050	150	E
8 5 4 0 → 8 4 5 0	3970997.405	0.173	150	E
3 2 1 0 → 2 1 2 0	3977046.481	0.343	150	E
7 2 5 0 → 6 3 4 0	4000164.750	0.037	150	E
9 5 5 0 → 9 4 6 0	4020094.138	-0.019	150	E
10 4 7 0 → 10 3 8 0	4053426.066	-0.042	150	E
9 3 7 0 → 9 2 8 0	4072555.267	0.126	150	E
10 5 6 0 → 10 4 7 0	4118633.703	-0.212	150	E
8 1 7 0 → 8 0 8 0	4161918.741	0.011	150	E
7 0 7 0 → 6 1 6 0	4166851.176	0.109	150	E
7 1 7 0 → 6 0 6 0	4190576.643	-0.093	150	E
5 2 4 0 → 4 1 3 0	4218430.618	0.050	150	E
8 2 7 0 → 8 1 8 0	4240191.823	0.718	150	E
11 5 7 0 → 11 4 8 0	4279695.925	0.241	150	E
10 2 8 0 → 10 1 9 0	4345505.100	0.161	150	E
11 6 5 0 → 11 5 6 0	4348518.162	-0.500	150	E
12 3 9 0 → 12 2 10 0	4366791.768	-0.313	150	E
11 4 8 0 → 11 3 9 0	4435759.411	0.550	150	E
3 3 0 0 → 3 0 3 0	4456621.984	-0.411	150	E
3 3 1 0 → 2 2 0 0	4468569.050	-0.084	150	E
3 3 0 0 → 2 2 1 0	4512384.121	-0.045	150	E
10 6 4 0 → 10 5 5 0	4519563.921	-0.217	150	E
7 1 6 0 → 6 2 5 0	4535939.553	-0.092	150	E
10 3 8 0 → 10 2 9 0	4571661.011	0.146	150	E
6 2 5 0 → 5 1 4 0	4600431.452	0.214	150	E
9 6 3 0 → 9 5 4 0	4619371.406	-0.203	150	E
8 6 2 0 → 8 5 3 0	4668678.294	-0.098	150	E
10 6 5 0 → 10 5 6 0	4684382.106	-0.187	150	E
9 6 4 0 → 9 5 5 0	4684697.855	0.145	150	E
7 6 1 0 → 7 5 2 0	4687526.543	-0.086	150	E
6 6 0 0 → 6 5 1 0	4689524.212	-0.153	150	E

Table 3—Continued

$J''K''_aK''_cV'' \rightarrow J'K'_aK'_cV'$	Frequency (MHz)	O-C (MHz)	Unc.(kHz)	Ref.
8 6 3 0 → 8 5 4 0	4690093.784	-0.050	150	E
6 6 1 0 → 6 5 2 0	4690528.924	-0.033	150	E
7 6 2 0 → 7 5 3 0	4693044.499	0.156	150	E
8 0 8 0 → 7 1 7 0	4724263.773	-0.037	150	E
8 1 8 0 → 7 0 7 0	4734296.171	0.420	150	E
9 1 8 0 → 9 0 9 0	4764038.870	-0.186	150	E
9 2 8 0 → 9 1 9 0	4801938.995	0.088	150	E
9 3 6 0 → 8 4 5 0	4802992.161	0.065	150	E
4 3 1 0 → 4 0 4 0	4850334.680	-0.133	150	E
12 4 9 0 → 12 3 10 0	4869963.371	-0.183	150	E

[A]Pearson et al. 1991

[B]Pearson 1995

[C]This Work

[D]Belov 1996

[E]Matsushima et al. 1995

Table 4. Predicted THz Water Transitions and Intensities

Transition	ν_{ab}(MHz)	Unc.	E_l(cm^{-1})	$\mu^2 S$	I(50 K)	I(200 K)	I(800 K)	I(1500 K)
4 2 2 5 1 5 010	2160.039	0.061	1922.8290	0.3861	2.374(-33)	5.093(-10)	4.080(-06)	1.093(-05)
9 3 6 10 2 9 010	7257.123	0.154	2904.4283	1.3478	3.683(-48)	1.466(-12)	2.345(-06)	1.432(-05)
4 2 3 3 3 0 010	12008.798	0.029	1907.6157	1.3443	2.267(-32)	3.155(-09)	2.330(-05)	6.164(-05)
6 1 6 5 2 3 000	22235.117	0.010	446.5107	0.5975	2.787(-09)	2.143(-04)	5.971(-04)	4.634(-04)
5 3 2 4 4 1 010	26834.241	0.028	2129.5992	1.2204	1.711(-35)	1.425(-09)	3.492(-05)	1.113(-04)
4 1 4 3 2 1 010	67803.990	0.036	1819.3351	1.4393	2.965(-30)	3.340(-08)	1.540(-04)	3.784(-04)
4 4 0 5 3 3 010	96260.851	0.055	2126.4077	0.3994	6.605(-35)	5.188(-09)	1.257(-04)	4.000(-04)
2 2 0 3 1 3 010	119996.136	0.059	1739.4837	0.3630	8.993(-29)	1.043(-07)	3.141(-04)	7.224(-04)
3 1 3 2 2 0 000	183310.030	0.013	136.1639	0.3501	1.473(-03)	1.616(-02)	8.561(-03)	5.132(-03)
5 5 1 6 4 2 010	209118.382	0.068	2399.1654	0.3508	7.369(-39)	1.563(-09)	1.667(-04)	6.677(-04)
5 5 0 6 4 3 010	232686.556	0.072	2398.3815	1.0503	8.321(-39)	1.744(-09)	1.856(-04)	7.433(-04)
14 4 10 15 3 13 000	247440.147	0.130	2872.5805	0.4090	3.432(-46)	6.109(-11)	8.407(-05)	5.014(-04)
13 6 8 14 3 11 000	259952.613	0.092	2739.4285	0.4405	4.304(-44)	1.670(-10)	1.122(-04)	5.984(-04)
6 6 1 7 5 2 010	293664.398	0.080	2724.1671	0.9482	8.259(-44)	2.097(-10)	1.301(-04)	6.856(-04)
6 6 0 7 5 3 010	297439.414	0.080	2724.0414	0.3160	8.385(-44)	2.125(-10)	1.318(-04)	6.945(-04)
10 2 9 9 3 6 000	321225.656	0.025	1282.9191	0.9915	2.909(-21)	7.279(-06)	1.900(-03)	2.987(-03)
5 1 5 4 2 2 000	325152.935	0.011	315.7795	0.3150	3.769(-06)	7.741(-03)	1.095(-02)	7.645(-03)
5 2 3 6 1 6 010	336227.931	0.093	2042.7533	0.7731	4.075(-33)	3.215(-08)	5.068(-04)	1.508(-03)
4 1 4 3 2 1 000	380197.366	0.011	212.1564	1.2760	1.777(-04)	1.895(-02)	1.540(-02)	9.865(-03)
10 3 7 11 2 10 000	390134.641	0.041	1525.1360	0.2468	5.593(-25)	1.535(-06)	1.489(-03)	2.873(-03)
8 5 4 7 6 1 010	425689.291	0.080	2905.4335	2.4896	1.639(-46)	8.124(-11)	1.356(-04)	8.335(-04)
7 5 3 6 6 0 000	437346.651	0.017	1045.0583	0.3325	1.930(-17)	5.411(-05)	3.953(-03)	5.100(-03)
6 4 3 5 5 0 000	439150.871	0.016	742.0763	1.1077	1.047(-12)	4.804(-04)	6.845(-03)	6.847(-03)
8 5 3 7 6 2 010	440737.706	0.081	2905.4306	0.8307	1.683(-46)	8.396(-11)	1.403(-04)	8.627(-04)
7 5 2 6 6 1 000	443018.312	0.016	1045.0579	0.9980	1.949(-17)	5.478(-05)	4.004(-03)	5.165(-03)
4 2 3 3 3 0 000	448001.134	0.014	285.4186	1.3850	1.446(-05)	1.308(-02)	1.587(-02)	1.082(-02)
4 2 2 3 3 1 010	463170.703	0.082	1907.4514	0.5251	6.798(-31)	1.155(-07)	8.870(-04)	2.361(-03)
6 4 2 5 5 1 000	470889.003	0.016	742.0730	0.3704	1.103(-12)	5.132(-04)	7.333(-03)	7.339(-03)
5 3 3 4 4 0 000	474689.257	0.016	488.1342	0.4200	1.029(-08)	3.213(-03)	1.167(-02)	9.438(-03)
6 2 4 7 1 7 000	488491.072	0.012	586.4792	0.1275	3.056(-10)	1.627(-03)	1.006(-02)	8.836(-03)
7 4 4 6 5 1 010	498502.349	0.079	2552.8797	0.8950	5.934(-41)	1.192(-09)	2.987(-04)	1.367(-03)
8 6 3 7 7 0 000	503568.837	0.039	1394.8142	0.9250	7.368(-23)	4.993(-06)	2.422(-03)	4.194(-03)
8 6 2 7 7 1 000	504482.999	0.039	1394.8141	0.3084	7.378(-23)	5.002(-06)	2.426(-03)	4.201(-03)
14 3 12 13 4 9 000	530342.750	0.111	2533.7932	1.4612	1.233(-40)	1.449(-09)	3.286(-04)	1.481(-03)
5 2 4 4 3 1 010	546690.698	0.070	2005.9170	0.9307	2.221(-32)	6.647(-08)	8.749(-04)	2.532(-03)
1 1 0 1 0 1 000	556935.988	0.009	23.7944	15.3568	2.071(-01)	1.054(-01)	3.148(-02)	1.726(-02)
12 6 7 13 3 10 000	571914.121	0.093	2414.7234	0.9787	9.422(-39)	3.662(-09)	4.384(-04)	1.789(-03)
7 4 3 6 5 2 010	578057.280	0.085	2552.8572	2.7059	6.599(-41)	1.369(-09)	3.456(-04)	1.583(-03)
9 2 8 8 3 5 010	593708.689	0.117	2670.7896	0.6418	9.665(-43)	6.009(-10)	2.870(-04)	1.452(-03)
6 3 4 5 4 1 010	595079.958	0.087	2251.8625	2.9024	3.390(-36)	1.226(-08)	6.110(-04)	2.175(-03)

Table 4—Continued

Transition	ν_{ab}(MHz)	Unc.	E_l(cm^{-1})	$\mu^2 S$	I(50 K)	I(200 K)	I(800 K)	I(1500 K)
5 3 2 4 4 1 000	620701.115	0.016	488.1077	1.2940	1.245(-08)	4.131(-03)	1.519(-02)	1.231(-02)
9 7 3 8 8 0 000	645766.054	0.063	1789.0428	0.2940	6.083(-29)	3.694(-07)	1.522(-03)	3.676(-03)
9 7 2 8 8 1 000	645905.564	0.063	1789.0428	0.8821	6.084(-29)	3.695(-07)	1.522(-03)	3.677(-03)
1 1 0 1 0 1 010	658006.475	0.063	1618.5571	14.8354	2.836(-26)	1.281(-06)	2.106(-03)	4.411(-03)
2 1 1 2 0 2 000	752033.132	0.010	70.0908	7.0636	4.777(-02)	9.972(-02)	3.889(-02)	2.223(-02)
11 5 7 12 2 10 000	766793.580	0.103	1960.2074	0.3179	1.438(-31)	1.262(-07)	1.324(-03)	3.697(-03)
10 5 6 11 2 9 000	841050.473	0.069	1690.6644	0.7964	2.467(-27)	9.544(-07)	2.352(-03)	5.246(-03)
12 5 8 13 2 11 000	854050.433	0.152	2246.8848	1.0280	5.094(-36)	1.770(-08)	8.780(-04)	3.124(-03)
2 1 1 2 0 2 010	859965.421	0.050	1664.9646	6.9909	6.299(-27)	1.171(-06)	2.517(-03)	5.496(-03)
10 8 3 9 9 0 000	863837.022	0.209	2225.4692	0.8630	1.108(-35)	2.086(-08)	9.227(-04)	3.224(-03)
10 8 2 9 9 1 000	863857.787	0.209	2225.4692	0.2877	1.108(-35)	2.086(-08)	9.227(-04)	3.225(-03)
2 0 2 1 1 1 010	899301.984	0.114	1634.9671	2.3946	1.900(-26)	1.513(-06)	2.775(-03)	5.911(-03)
6 2 4 7 1 7 010	902397.810	0.109	2181.0899	0.1679	5.602(-35)	2.985(-08)	1.043(-03)	3.513(-03)
3 1 2 2 2 1 010	902609.359	0.116	1742.3056	2.8115	4.008(-28)	7.014(-07)	2.296(-03)	5.352(-03)
9 2 8 8 3 5 000	906205.939	0.019	1050.1577	0.4767	2.608(-17)	1.023(-04)	8.004(-03)	1.044(-02)
4 2 2 3 3 1 000	916171.509	0.014	285.2193	0.5678	2.336(-05)	2.536(-02)	3.202(-02)	2.197(-02)
6 2 5 5 3 2 010	923113.564	0.092	2130.4943	3.5914	3.501(-34)	4.384(-08)	1.168(-03)	3.771(-03)
6 3 3 5 4 2 010	926187.453	0.097	2251.6953	1.0271	4.483(-36)	1.839(-08)	9.420(-04)	3.368(-03)
8 2 7 7 3 4 010	968047.499	0.115	2462.8752	2.7134	2.307(-39)	4.186(-09)	6.726(-04)	2.873(-03)
5 2 4 4 3 1 000	970315.097	0.013	383.8425	0.9219	6.938(-07)	1.313(-02)	2.835(-02)	2.115(-02)
2 0 2 1 1 1 000	987926.549	0.012	37.1371	2.5830	1.826(-01)	1.616(-01)	5.383(-02)	3.003(-02)
13 5 9 14 2 12 000	1068679.420	0.241	2550.8825	0.3476	1.024(-40)	2.425(-09)	6.319(-04)	2.910(-03)
7 2 6 6 3 3 010	1077763.388	0.111	2282.5896	1.1504	1.596(-36)	1.683(-08)	1.032(-03)	3.796(-03)
3 1 2 3 0 3 000	1097364.905	0.012	136.7617	22.2672	5.346(-03)	8.655(-02)	4.982(-02)	3.026(-02)
11 6 6 12 3 9 000	1101130.602	0.086	2105.8679	0.2030	9.295(-34)	6.116(-08)	1.448(-03)	4.592(-03)
9 5 5 10 2 8 000	1109597.594	0.040	1437.9686	0.1875	2.532(-23)	7.518(-06)	4.850(-03)	8.781(-03)
1 1 1 0 0 0 000	1113342.917	0.008	0.0000	3.4126	7.371(-01)	2.345(-01)	6.461(-02)	3.499(-02)
7 2 5 8 1 8 000	1146621.322	0.015	744.1627	0.2674	1.772(-12)	1.138(-03)	1.743(-02)	1.764(-02)
3 1 2 2 2 1 000	1153126.676	0.014	134.9016	3.1104	5.852(-03)	9.159(-02)	5.244(-02)	3.183(-02)
11 3 8 12 2 11 000	1153370.911	0.086	1774.7511	0.6005	1.414(-28)	6.895(-07)	2.747(-03)	6.603(-03)
11 9 3 10 10 0 000	1155166.484	0.477	2701.8885	0.2880	4.648(-43)	8.759(-10)	5.193(-04)	2.718(-03)
11 9 2 10 10 1 000	1155169.558	0.477	2701.8885	0.8641	4.648(-43)	8.759(-10)	5.193(-04)	2.718(-03)
6 3 4 5 4 1 000	1158323.892	0.016	610.3412	3.0156	2.193(-10)	3.007(-03)	2.240(-02)	2.026(-02)
3 2 1 3 1 2 000	1162911.700	0.010	173.3658	26.0030	1.473(-03)	6.996(-02)	4.934(-02)	3.093(-02)
8 5 4 7 6 1 000	1168358.517	0.020	1216.1945	2.6178	7.558(-20)	3.877(-05)	7.596(-03)	1.143(-02)
7 4 4 6 5 1 000	1172525.859	0.019	888.6326	0.9410	9.912(-15)	4.104(-04)	1.374(-02)	1.570(-02)
8 5 3 7 6 2 000	1190828.892	0.020	1216.1898	0.8742	7.625(-20)	3.942(-05)	7.737(-03)	1.164(-02)
1 1 1 0 0 0 010	1205789.303	0.107	1594.7463	3.2974	9.355(-26)	2.616(-06)	3.964(-03)	8.197(-03)
4 2 2 4 1 3 000	1207638.712	0.012	275.4970	12.4015	3.803(-05)	3.467(-02)	4.258(-02)	2.910(-02)
3 1 2 3 0 3 010	1214661.769	0.057	1731.8967	22.7706	6.760(-28)	9.814(-07)	3.119(-03)	7.239(-03)

Table 4—Continued

Transition	ν_{ab}(MHz)	Unc.	E_l(cm^{-1})	$\mu^2 S$	I(50 K)	I(200 K)	I(800 K)	I(1500 K)
8 4 5 7 5 2 010	1215067.641	0.119	2724.1671	4.6214	2.134(-43)	7.795(-10)	5.238(-04)	2.795(-03)
9 6 4 8 7 1 000	1215801.736	0.059	1590.6907	0.8247	1.086(-25)	2.713(-06)	4.025(-03)	8.296(-03)
9 6 3 8 7 2 000	1219944.374	0.059	1590.6900	2.4750	1.088(-25)	2.721(-06)	4.038(-03)	8.324(-03)
7 3 5 6 4 2 010	1222823.607	0.103	2399.1654	1.5476	2.555(-38)	8.121(-09)	9.455(-04)	3.842(-03)
2 2 0 2 1 1 000	1228788.840	0.011	95.1759	4.3124	2.514(-02)	1.288(-01)	5.988(-02)	3.519(-02)
13 3 11 12 4 8 000	1271472.972	0.119	2205.6527	0.6222	2.740(-35)	3.379(-08)	1.390(-03)	4.806(-03)
7 4 3 6 5 2 000	1278265.923	0.018	888.5987	2.8582	1.031(-14)	4.422(-04)	1.493(-02)	1.709(-02)
8 2 7 7 3 4 000	1296411.049	0.015	842.3566	2.1147	5.471(-14)	6.242(-04)	1.645(-02)	1.811(-02)
8 4 5 9 1 8 000	1307963.287	0.023	1079.0796	0.4935	1.101(-17)	1.145(-04)	1.084(-02)	1.456(-02)
6 2 5 5 3 2 000	1322064.783	0.013	508.8121	3.3216	8.956(-09)	6.993(-03)	3.054(-02)	2.542(-02)
10 7 4 9 8 1 000	1335279.326	0.128	2009.8051	2.3935	3.206(-32)	1.441(-07)	2.073(-03)	6.084(-03)
10 7 3 9 8 2 000	1335984.734	0.128	2009.8050	0.7978	3.207(-32)	1.442(-07)	2.074(-03)	6.087(-03)
7 4 4 8 1 7 000	1344676.176	0.017	882.8903	0.1315	1.292(-14)	4.810(-04)	1.584(-02)	1.806(-02)
14 5 10 15 2 13 000	1378167.571	0.378	2872.2742	1.0248	1.092(-45)	2.990(-10)	4.530(-04)	2.744(-03)
13 7 7 14 4 10 000	1386269.011	0.257	2880.8342	0.1842	8.046(-46)	2.826(-10)	4.486(-04)	2.737(-03)
3 2 1 3 1 2 010	1406675.550	0.091	1772.4134	24.2006	1.672(-28)	8.309(-07)	3.340(-03)	8.039(-03)
5 2 3 5 1 4 000	1410617.988	0.012	399.4575	42.9566	4.694(-07)	1.622(-02)	3.956(-02)	3.008(-02)
4 2 2 4 1 3 010	1421957.576	0.106	1875.4697	11.8469	4.123(-30)	3.995(-07)	2.803(-03)	7.360(-03)
8 4 4 7 5 3 010	1428471.994	0.129	2724.0414	1.5781	2.290(-43)	8.953(-10)	6.121(-04)	3.276(-03)
9 4 6 10 1 9 000	1435008.375	0.040	1293.0181	0.1777	5.194(-21)	2.658(-05)	8.062(-03)	1.298(-02)
7 2 6 6 3 3 000	1440781.665	0.013	661.5489	0.9729	3.808(-11)	2.506(-03)	2.520(-02)	2.389(-02)
5 2 3 4 3 2 010	1473570.467	0.113	2004.8157	4.1321	3.984(-32)	1.623(-07)	2.299(-03)	6.731(-03)
2 2 0 2 1 1 010	1494057.486	0.081	1693.6499	3.9989	2.907(-27)	1.540(-06)	4.076(-03)	9.196(-03)
11 8 4 10 9 1 000	1529130.687	0.249	2471.2550	0.7896	2.087(-39)	5.839(-09)	1.029(-03)	4.462(-03)
11 8 3 10 9 2 000	1529245.716	0.248	2471.2550	2.3689	2.087(-39)	5.840(-09)	1.029(-03)	4.462(-03)
6 3 3 5 4 2 000	1541967.050	0.015	610.1144	1.0979	2.482(-10)	3.838(-03)	2.949(-02)	2.681(-02)
6 4 3 7 1 6 000	1574232.067	0.014	704.2140	0.2449	8.469(-12)	1.984(-03)	2.540(-02)	2.500(-02)
5 2 3 5 1 4 010	1592068.265	0.116	2000.8630	42.7077	4.718(-32)	1.780(-07)	2.493(-03)	7.287(-03)
8 5 4 9 2 7 000	1596252.461	0.023	1201.9215	0.3118	1.429(-19)	5.592(-05)	1.051(-02)	1.572(-02)
4 1 3 4 0 4 000	1602219.342	0.011	222.0528	6.9404	2.901(-04)	6.461(-02)	6.147(-02)	4.039(-02)
3 0 3 2 1 2 010	1643919.328	0.109	1677.0614	16.5369	5.453(-27)	1.877(-06)	4.601(-03)	1.026(-02)
7 2 5 8 1 8 010	1646632.434	0.122	2337.6668	0.3481	2.613(-37)	1.622(-08)	1.404(-03)	5.451(-03)
2 2 1 2 1 2 000	1661007.762	0.011	79.4964	8.5508	4.949(-02)	1.856(-01)	8.221(-02)	4.796(-02)
2 1 2 1 0 1 000	1669904.752	0.009	23.7944	15.3477	3.676(-01)	2.782(-01)	9.133(-02)	5.085(-02)
10 4 7 11 1 10 000	1693469.742	0.071	1524.8479	0.5314	1.314(-24)	5.749(-06)	6.223(-03)	1.222(-02)
4 3 2 5 0 5 000	1713882.952	0.012	325.3479	0.1144	7.213(-06)	3.246(-02)	5.443(-02)	3.906(-02)
3 0 3 2 1 2 000	1716769.533	0.011	79.4964	17.8475	4.999(-02)	1.906(-01)	8.483(-02)	4.952(-02)
5 3 3 6 0 6 000	1716956.616	0.013	446.6966	0.0561	9.177(-08)	1.358(-02)	4.383(-02)	3.482(-02)
4 1 3 4 0 4 010	1739351.281	0.066	1817.4512	7.2464	3.557(-29)	7.158(-07)	3.771(-03)	9.470(-03)
8 3 6 7 4 3 010	1740397.563	0.133	2572.1391	5.9464	5.777(-41)	3.141(-09)	9.710(-04)	4.594(-03)

Table 4—Continued

Transition	ν_{ab}(MHz)	Unc.	E_l(cm^{-1})	$\mu^2 S$	I(50 K)	I(200 K)	I(800 K)	I(1500 K)
2 1 2 1 0 1 0 1 0	1753915.445	0.111	1618.5571	14.8282	4.562(-26)	3.014(-06)	5.435(-03)	1.155(-02)
6 3 3 6 2 4 0 0 0	1762042.660	0.012	602.7735	16.3527	3.372(-10)	4.512(-03)	3.393(-02)	3.075(-02)
7 3 5 6 4 2 0 0 0	1766198.743	0.015	757.7802	1.5662	1.278(-12)	1.482(-03)	2.573(-02)	2.656(-02)
12 9 4 11 10 1 0 0 0	1794632.021	0.522	2972.8273	2.3932	3.207(-47)	1.803(-10)	4.863(-04)	3.223(-03)
12 9 3 11 10 2 0 0 0	1794650.403	0.523	2972.8273	0.7978	3.207(-47)	1.803(-10)	4.863(-04)	3.223(-03)
6 2 4 6 1 5 0 0 0	1794788.923	0.011	542.9058	14.3411	2.920(-09)	7.043(-03)	3.845(-02)	3.315(-02)
7 3 4 7 2 5 0 0 0	1797158.733	0.013	782.4098	60.0582	5.298(-13)	1.259(-03)	2.502(-02)	2.638(-02)
4 1 3 3 2 2 0 1 0	1849183.592	0.113	1813.7876	2.5494	4.128(-29)	7.718(-07)	4.022(-03)	1.009(-02)
10 6 5 11 3 8 0 0 0	1851205.596	0.064	1813.2234	0.3073	4.214(-29)	7.756(-07)	4.031(-03)	1.010(-02)
5 3 2 5 2 3 0 0 0	1867748.467	0.011	446.5107	35.1483	9.462(-08)	1.455(-02)	4.748(-02)	3.780(-02)
8 2 6 9 1 9 0 0 0	1879750.121	0.020	920.2100	0.0691	3.774(-15)	4.841(-04)	2.038(-02)	2.415(-02)
6 3 4 7 0 7 0 0 0	1880752.361	0.015	586.2435	0.1898	6.222(-10)	5.352(-03)	3.717(-02)	3.328(-02)
8 4 5 7 5 2 0 0 0	1884887.913	0.017	1059.8354	4.8219	2.488(-17)	1.777(-04)	1.589(-02)	2.118(-02)
3 3 1 4 0 4 0 0 0	1893686.545	0.014	222.0528	0.0143	3.047(-04)	7.392(-02)	7.203(-02)	4.751(-02)
9 4 6 8 5 3 0 1 0	1894418.074	0.164	2920.1320	2.2030	2.166(-46)	2.749(-10)	5.627(-04)	3.573(-03)
9 5 5 8 6 2 0 0 0	1898852.244	0.024	1411.6419	1.5429	7.961(-23)	1.422(-05)	8.501(-03)	1.522(-02)
12 3 9 13 2 12 0 0 0	1903497.257	0.161	2042.3741	0.1737	1.117(-32)	1.525(-07)	2.740(-03)	8.331(-03)
12 3 10 11 4 7 0 0 0	1903643.698	0.101	1899.0082	2.5376	1.940(-30)	4.278(-07)	3.547(-03)	9.560(-03)
5 2 3 4 3 2 0 0 0	1918485.441	0.012	382.5169	4.5857	9.521(-07)	2.354(-02)	5.464(-02)	4.125(-02)
3 2 2 3 1 3 0 0 0	1919359.520	0.010	142.2785	4.4203	5.391(-03)	1.326(-01)	8.421(-02)	5.196(-02)
10 6 5 9 7 2 0 0 0	1930215.966	0.074	1810.5879	4.4555	4.684(-29)	8.170(-07)	4.213(-03)	1.055(-02)
7 3 4 6 4 3 0 1 0	1933474.781	0.118	2398.3815	5.4505	3.080(-38)	1.192(-08)	1.466(-03)	6.011(-03)
10 6 4 9 7 3 0 0 0	1945009.917	0.077	1810.5833	1.4864	4.694(-29)	8.219(-07)	4.243(-03)	1.062(-02)
6 2 4 6 1 5 0 1 0	1946460.306	0.120	2146.2637	14.8293	2.678(-34)	7.350(-08)	2.322(-03)	7.705(-03)
2 2 1 2 1 2 0 1 0	1955971.738	0.071	1677.0614	8.2606	5.728(-27)	2.157(-06)	5.424(-03)	1.214(-02)
9 5 4 8 6 3 0 0 0	1969214.416	0.024	1411.6114	4.6568	8.044(-23)	1.464(-05)	8.798(-03)	1.577(-02)
5 4 2 6 1 5 0 0 0	2014864.532	0.014	542.9058	0.0334	3.009(-09)	7.716(-03)	4.288(-02)	3.709(-02)
8 3 5 8 2 6 0 0 0	2015982.847	0.015	982.9117	21.5977	4.026(-16)	3.258(-04)	1.945(-02)	2.433(-02)
11 7 5 10 8 2 0 0 0	2024457.394	0.165	2254.2844	1.4553	5.552(-36)	3.484(-08)	1.984(-03)	7.217(-03)
11 7 4 10 8 3 0 0 0	2027255.529	0.164	2254.2837	4.3666	5.554(-36)	3.488(-08)	1.986(-03)	7.226(-03)
4 3 1 4 2 2 0 0 0	2040476.759	0.011	315.7795	7.4297	1.066(-05)	3.993(-02)	6.529(-02)	4.668(-02)
11 4 8 12 1 11 0 0 0	2050980.055	0.124	1774.6163	0.1699	1.734(-28)	1.110(-06)	4.759(-03)	1.158(-02)
4 1 3 3 2 2 0 0 0	2074432.382	0.012	206.3014	2.8729	5.491(-04)	8.890(-02)	8.074(-02)	5.269(-02)
9 3 7 8 4 4 0 1 0	2090772.019	0.158	2771.6901	2.1278	4.624(-44)	8.638(-10)	8.064(-04)	4.532(-03)
7 3 4 7 2 5 0 1 0	2107022.663	0.125	2392.5925	57.1509	3.871(-38)	1.329(-08)	1.606(-03)	6.569(-03)
6 3 3 6 2 4 0 1 0	2140487.032	0.100	2211.1906	15.0451	2.649(-35)	4.959(-08)	2.259(-03)	7.938(-03)
8 4 4 7 5 3 0 0 0	2162370.498	0.017	1059.6466	1.6709	2.588(-17)	1.980(-04)	1.809(-02)	2.419(-02)
3 1 3 2 0 2 0 0 0	2164132.001	0.010	70.0908	7.3550	7.438(-02)	2.447(-01)	1.073(-01)	6.255(-02)
7 3 5 8 0 8 0 0 0	2177409.704	0.016	744.0637	0.0628	2.205(-12)	1.927(-03)	3.212(-02)	3.296(-02)
12 8 5 11 9 2 0 0 0	2191225.490	0.313	2740.4208	4.3644	1.438(-43)	1.121(-09)	8.914(-04)	4.887(-03)

Table 4—Continued

Transition	ν_{ab}(MHz)	Unc.	E_l(cm^{-1})	$\mu^2 S$	I(50 K)	I(200 K)	I(800 K)	I(1500 K)
12 8 4 11 9 3 000	2191723.253	0.308	2740.4207	1.4549	1.438(-43)	1.121(-09)	8.916(-04)	4.888(-03)
3 3 0 3 2 1 000	2196345.790	0.012	212.1564	11.3059	4.503(-04)	8.904(-02)	8.429(-02)	5.537(-02)
10 3 8 9 4 5 010	2217265.507	0.200	2998.7663	5.8441	1.328(-17)	1.764(-10)	5.663(-04)	3.858(-03)
5 1 4 5 0 5 000	2221750.406	0.012	325.3479	19.4139	7.696(-06)	3.978(-02)	6.951(-02)	5.022(-02)
3 2 2 3 1 3 010	2227574.164	0.053	1739.4837	4.3281	6.244(-28)	1.522(-06)	5.477(-03)	1.297(-02)
3 1 3 2 0 2 010	2234026.771	0.095	1664.9646	7.0483	9.116(-27)	2.607(-06)	6.280(-03)	1.397(-02)
8 3 6 7 4 3 000	2244811.054	0.017	931.2371	5.7304	2.644(-15)	5.130(-04)	2.360(-02)	2.837(-02)
8 3 5 8 2 6 010	2247746.017	0.145	2595.8129	21.5405	2.624(-41)	3.235(-09)	1.184(-03)	5.754(-03)
4 2 3 4 1 4 000	2264149.558	0.011	224.8384	15.9562	2.871(-04)	8.316(-02)	8.477(-02)	5.632(-02)
5 3 2 5 2 3 010	2294179.491	0.089	2053.9687	32.0786	7.677(-33)	1.620(-07)	3.198(-03)	9.868(-03)
8 4 5 9 1 8 010	2296935.416	0.148	2688.0799	0.4914	9.538(-43)	1.693(-09)	1.023(-03)	5.378(-03)
7 5 3 8 2 6 000	2300455.716	0.016	982.9117	0.0419	4.140(-16)	3.603(-04)	2.201(-02)	2.764(-02)
9 4 5 9 3 6 000	2317882.104	0.019	1282.9191	71.7068	8.531(-21)	4.186(-05)	1.292(-02)	2.088(-02)
4 0 4 3 1 3 010	2337406.476	0.090	1739.4837	9.0340	6.301(-28)	1.578(-06)	5.729(-03)	1.358(-02)
7 2 5 7 1 6 000	2344250.362	0.013	704.2140	40.4877	9.379(-12)	2.713(-03)	3.697(-02)	3.677(-02)
10 4 6 10 3 7 000	2347482.039	0.034	1538.1495	27.4357	8.808(-25)	6.737(-06)	8.261(-03)	1.655(-02)
11 3 9 10 4 6 000	2356835.957	0.068	1616.4530	1.1816	5.272(-26)	3.847(-06)	7.203(-03)	1.541(-02)
3 3 1 3 2 2 000	2365899.585	0.012	206.3014	3.5691	5.637(-04)	9.820(-02)	9.130(-02)	5.982(-02)
12 7 6 13 4 9 000	2368560.214	0.188	2533.7932	0.2686	2.466(-40)	5.256(-09)	1.390(-03)	6.423(-03)
9 4 5 8 5 4 010	2372359.855	0.165	2919.6329	7.0506	2.316(-46)	3.279(-10)	6.955(-04)	4.443(-03)
7 4 4 8 1 7 010	2372974.395	0.136	2490.3540	0.1207	1.177(-39)	7.194(-09)	1.505(-03)	6.708(-03)
4 0 4 3 1 3 000	2391572.560	0.011	142.2785	9.6574	5.650(-03)	1.569(-01)	1.035(-01)	6.427(-02)
5 1 4 5 0 5 010	2401232.209	0.091	1920.7665	20.2743	9.323(-31)	4.369(-07)	4.240(-03)	1.172(-02)
9 4 6 10 1 9 010	2403645.199	0.170	2903.1460	0.1882	4.201(-46)	3.728(-10)	7.252(-04)	4.571(-03)
9 3 6 9 2 7 000	2428247.324	0.022	1201.9215	63.7149	1.584(-19)	7.760(-05)	1.561(-02)	2.360(-02)
8 4 4 8 3 5 000	2446843.367	0.015	1050.1577	19.1211	3.726(-17)	2.325(-04)	2.065(-02)	2.750(-02)
4 3 2 4 2 3 000	2462932.987	0.010	300.3623	19.0025	1.926(-05)	5.142(-02)	8.003(-02)	5.681(-02)
12 4 9 13 1 12 000	2477509.147	0.197	2042.3106	0.4816	1.183(-32)	1.865(-07)	3.508(-03)	1.075(-02)
7 2 5 7 1 6 010	2484151.505	0.128	2309.7302	42.7282	7.866(-37)	2.729(-08)	2.174(-03)	8.336(-03)
4 3 1 4 2 2 010	2488754.367	0.087	1922.9011	6.8665	8.685(-31)	4.417(-07)	4.366(-03)	1.210(-02)
8 2 6 9 1 9 010	2501384.400	0.160	2512.3757	0.0876	5.378(-40)	6.383(-09)	1.520(-03)	6.909(-03)
4 3 2 5 0 5 010	2519730.008	0.097	1920.7665	0.1086	9.396(-31)	4.526(-07)	4.434(-03)	1.227(-02)
9 3 7 8 4 4 000	2531917.714	0.021	1131.7756	1.9010	1.989(-18)	1.325(-04)	1.841(-02)	2.628(-02)
5 3 3 6 0 6 010	2537059.710	0.108	2041.7805	0.0574	1.211(-32)	1.905(-07)	3.589(-03)	1.100(-02)
6 2 4 5 3 3 010	2541727.556	0.116	2126.4077	2.6323	5.769(-34)	1.037(-07)	3.088(-03)	1.016(-02)
9 4 6 8 5 3 000	2547436.478	0.023	1255.9115	2.2607	2.290(-20)	5.450(-05)	1.481(-02)	2.347(-02)
7 3 4 6 4 3 000	2567177.028	0.014	756.7248	5.9475	1.440(-12)	1.988(-03)	3.660(-02)	3.816(-02)
11 4 7 11 3 8 000	2571762.517	0.067	1813.2234	86.2552	4.511(-29)	9.958(-07)	5.483(-03)	1.387(-02)
10 3 8 9 4 5 000	2575004.418	0.038	1360.2353	4.7652	5.380(-22)	2.593(-05)	1.240(-02)	2.145(-02)
8 3 6 9 0 9 000	2576644.138	0.020	920.1683	0.1768	4.030(-15)	6.151(-04)	2.737(-02)	3.274(-02)

Table 4—Continued

Transition	ν_{ab}(MHz)	Unc.	E_l(cm^{-1})	$\mu^2 S$	I(50 K)	I(200 K)	I(800 K)	I(1500 K)
9 3 6 9 2 7 010	2586380.182	0.173	2818.3980	66.2964	8.959(-45)	7.235(-10)	9.039(-04)	5.319(-03)
4 2 3 4 1 4 010	2590791.891	0.063	1821.5968	15.8430	3.342(-29)	9.426(-07)	5.437(-03)	1.386(-02)
13 3 10 14 2 13 000	2602481.851	0.244	2327.9140	0.4726	4.119(-37)	2.476(-08)	2.197(-03)	8.566(-03)
10 5 6 9 6 3 000	2618261.548	0.039	1631.3830	6.8434	3.134(-26)	3.732(-06)	7.730(-03)	1.681(-02)
9 2 7 10 1 10 000	2619333.979	0.044	1114.5499	0.1742	3.714(-18)	1.537(-04)	1.959(-02)	2.760(-02)
5 3 3 5 2 4 000	2630959.374	0.011	416.2087	8.4864	3.015(-07)	2.344(-02)	6.907(-02)	5.416(-02)
4 1 4 3 0 3 000	2640473.971	0.011	136.7617	30.7215	6.997(-03)	1.755(-01)	1.146(-01)	7.105(-02)
11 6 6 10 7 3 000	2645039.630	0.095	2054.3687	2.2430	7.744(-33)	1.793(-07)	3.647(-03)	1.131(-02)
3 3 0 3 2 1 010	2646587.083	0.062	1819.3351	10.6126	3.636(-29)	9.728(-07)	5.568(-03)	1.418(-02)
4 4 1 5 1 4 000	2657665.340	0.016	399.4575	0.0201	5.515(-07)	2.664(-02)	7.185(-02)	5.557(-02)
6 4 3 7 1 6 010	2657699.387	0.129	2309.7302	0.2041	7.945(-37)	2.865(-08)	2.314(-03)	8.894(-03)
7 4 3 7 3 4 000	2664570.784	0.013	842.3566	43.3807	6.652(-14)	1.103(-03)	3.247(-02)	3.643(-02)
5 2 4 5 1 5 000	2685638.921	0.011	326.6255	5.7894	7.585(-06)	4.532(-02)	8.270(-02)	6.019(-02)
4 1 4 3 0 3 010	2689141.309	0.090	1731.8967	29.2361	8.462(-28)	1.846(-06)	6.613(-03)	1.566(-02)
11 6 5 10 7 4 000	2689170.032	0.117	2054.3452	6.7504	7.768(-33)	1.814(-07)	3.703(-03)	1.149(-02)
3 3 1 4 0 4 010	2698138.154	0.098	1817.4512	0.0124	3.901(-29)	9.997(-07)	5.687(-03)	1.447(-02)
12 7 6 11 8 3 000	2714161.593	0.206	2522.2651	6.6791	3.812(-40)	6.305(-09)	1.610(-03)	7.401(-03)
12 7 5 11 8 4 000	2723413.666	0.224	2522.2613	2.2272	3.815(-40)	6.320(-09)	1.615(-03)	7.425(-03)
6 3 4 7 0 7 010	2730190.159	0.114	2180.6429	0.2054	8.283(-35)	7.393(-08)	2.992(-03)	1.033(-02)
2 2 1 1 1 0 000	2773976.526	0.008	42.3717	15.3993	2.100(-01)	3.584(-01)	1.421(-01)	8.155(-02)
5 1 4 4 2 3 010	2783473.884	0.116	1908.0163	14.8199	1.507(-30)	5.327(-07)	4.973(-03)	1.367(-02)
9 6 4 10 3 7 000	2790947.707	0.037	1538.1495	0.0417	9.040(-25)	7.637(-06)	9.696(-03)	1.954(-02)
10 5 5 9 6 4 000	2801857.636	0.042	1631.2455	2.3229	3.177(-26)	3.919(-06)	8.230(-03)	1.793(-02)
3 3 1 3 2 2 010	2807970.466	0.042	1813.7876	3.3920	4.473(-29)	1.056(-06)	5.939(-03)	1.508(-02)
9 4 5 9 3 6 010	2820925.179	0.168	2904.6704	65.4558	4.069(-46)	4.137(-10)	8.384(-04)	5.321(-03)
12 5 7 12 4 8 000	2848995.792	0.089	2205.6527	31.0801	3.387(-35)	6.363(-08)	2.974(-03)	1.050(-02)
13 5 8 13 4 9 000	2864256.164	0.161	2533.7932	103.587	2.535(-40)	6.026(-09)	1.657(-03)	7.706(-03)
6 3 4 6 2 5 000	2880025.294	0.013	552.9114	30.1032	2.232(-09)	9.346(-03)	5.870(-02)	5.180(-02)
6 1 5 6 0 6 000	2884278.885	0.012	446.6966	6.2551	1.019(-07)	2.009(-02)	7.115(-02)	5.743(-02)
6 4 2 6 3 3 000	2884941.040	0.011	661.5489	10.5528	4.485(-11)	4.283(-03)	4.836(-02)	4.675(-02)
4 3 2 4 2 3 010	2901971.683	0.052	1908.0163	18.1610	1.514(-30)	5.484(-07)	5.167(-03)	1.422(-02)
13 4 10 14 1 13 000	2947342.726	0.276	2327.8837	0.1516	4.188(-37)	2.704(-08)	2.463(-03)	9.649(-03)
6 2 4 5 3 3 000	2962111.192	0.013	503.9681	3.0060	1.302(-08)	1.355(-02)	6.577(-02)	5.576(-02)
2 2 0 1 1 1 000	2968748.520	0.008	37.1371	4.2551	2.555(-01)	3.901(-01)	1.526(-01)	8.744(-02)
5 1 4 4 2 3 000	2970800.440	0.012	300.3623	16.8476	1.974(-05)	5.874(-02)	9.511(-02)	6.798(-02)
5 0 5 4 1 4 010	2973033.566	0.081	1821.5968	37.7312	3.399(-29)	1.038(-06)	6.171(-03)	1.581(-02)
12 4 8 12 3 9 000	2991473.560	0.112	2105.8679	28.1269	1.233(-33)	1.349(-07)	3.722(-03)	1.211(-02)
11 5 6 11 4 7 000	2997538.796	0.062	1899.0082	78.8121	2.101(-30)	5.983(-07)	5.409(-03)	1.479(-02)
8 2 6 8 1 7 000	2998565.616	0.016	882.8903	12.7491	1.570(-14)	8.948(-04)	3.364(-02)	3.922(-02)
10 3 7 10 2 8 000	3003347.597	0.040	1437.9686	20.0636	3.347(-23)	1.652(-05)	1.242(-02)	2.307(-02)

Table 4—Continued

Transition	ν_{ab}(MHz)	Unc.	E_l(cm^{-1})	$\mu^2 S$	I(50 K)	I(200 K)	I(800 K)	I(1500 K)
15 4 12 14 5 9 000	3011981.501	0.433	2983.3963	1.3618	2.414(-47)	2.457(-10)	7.727(-04)	5.253(-03)
5 0 5 4 1 4 000	3013199.593	0.011	224.8384	39.9373	2.991(-04)	1.021(-01)	1.104(-01)	7.408(-02)
8 4 4 8 3 5 010	3024920.029	0.127	2670.7896	17.2661	1.847(-42)	2.335(-09)	1.361(-03)	7.118(-03)
8 5 4 9 2 7 010	3034945.506	0.169	2818.3980	0.2240	9.134(-45)	8.094(-10)	1.047(-03)	6.198(-03)
8 3 5 7 4 4 010	3036348.078	0.139	2569.5080	2.8420	7.059(-41)	4.852(-09)	1.639(-03)	7.873(-03)
5 2 4 5 1 5 010	3037605.104	0.085	1922.8290	5.8178	8.931(-31)	5.087(-07)	5.245(-03)	1.464(-02)
5 4 1 5 3 2 000	3043766.185	0.012	508.8121	21.4768	1.097(-08)	1.333(-02)	6.684(-02)	5.696(-02)
9 3 7 10 0 10 000	3048859.624	0.045	1114.5322	0.0542	3.784(-18)	1.710(-04)	2.252(-02)	3.191(-02)
2 2 1 1 1 0 010	3051880.708	0.113	1640.5059	14.8797	2.298(-26)	3.890(-06)	8.753(-03)	1.929(-02)
5 3 3 5 2 4 010	3065530.020	0.074	2024.1526	8.1968	2.336(-32)	2.469(-07)	4.408(-03)	1.340(-02)
7 3 5 8 0 8 010	3072608.565	0.119	2337.4633	0.0707	2.979(-37)	2.596(-08)	2.514(-03)	9.947(-03)
14 5 9 14 4 10 000	3074733.516	0.275	2880.8342	35.7516	9.679(-46)	5.211(-10)	9.469(-04)	5.911(-03)
10 4 7 9 5 4 000	3118999.242	0.039	1477.2974	8.2985	8.163(-24)	1.277(-05)	1.197(-02)	2.303(-02)
4 4 0 4 3 1 000	3126585.214	0.015	383.8425	3.7966	9.850(-07)	3.336(-02)	8.575(-02)	6.587(-02)
6 1 5 6 0 6 010	3132326.961	0.115	2041.7805	6.4769	1.241(-32)	2.207(-07)	4.355(-03)	1.345(-02)
5 1 5 4 0 4 000	3135010.989	0.011	222.0528	13.5189	3.319(-04)	1.070(-01)	1.150(-01)	7.713(-02)
9 4 5 8 5 4 000	3149876.967	0.019	1255.1667	7.5432	2.412(-20)	6.354(-05)	1.801(-02)	2.876(-02)
5 1 5 4 0 4 010	3159148.818	0.097	1817.4512	12.8548	3.969(-29)	1.115(-06)	6.570(-03)	1.682(-02)
5 4 2 6 1 5 010	3160759.885	0.128	2146.2637	0.0253	2.898(-34)	1.047(-07)	3.639(-03)	1.228(-02)
8 2 6 8 1 7 010	3161576.457	0.147	2490.3540	13.4260	1.221(-39)	8.811(-09)	1.960(-03)	8.827(-03)
4 4 1 4 3 2 000	3165532.793	0.015	382.5169	11.3298	1.034(-06)	3.396(-02)	8.693(-02)	6.674(-02)
6 2 5 6 1 6 000	3167578.134	0.011	447.2524	18.0370	1.008(-07)	2.132(-02)	7.742(-02)	6.276(-02)
5 4 2 5 3 3 000	3182186.801	0.012	503.9681	7.0043	1.311(-08)	1.422(-02)	7.021(-02)	5.970(-02)
6 5 2 7 2 5 000	3183463.594	0.016	782.4098	0.0344	5.860(-13)	1.919(-03)	4.257(-02)	4.572(-02)
7 3 5 7 2 6 000	3210358.118	0.014	709.6082	11.0338	8.044(-12)	3.259(-03)	4.889(-02)	4.942(-02)
6 4 3 6 3 4 000	3230146.418	0.012	648.9787	29.6233	7.126(-11)	5.061(-03)	5.483(-02)	5.269(-02)
14 3 11 15 2 14 000	3242105.141	0.345	2631.2835	0.1468	7.696(-42)	3.251(-09)	1.556(-03)	7.897(-03)
10 5 5 10 4 6 000	3245323.304	0.039	1616.4530	21.4177	5.489(-26)	4.819(-06)	9.665(-03)	2.092(-02)
2 2 0 1 1 1 010	3253324.891	0.127	1634.9671	4.2116	2.821(-26)	4.224(-06)	9.369(-03)	2.060(-02)
7 4 3 7 3 4 010	3275649.115	0.095	2462.8752	39.6415	3.292(-39)	1.099(-08)	2.127(-03)	9.372(-03)
11 5 7 10 6 4 000	3307403.060	0.072	1875.4618	3.0218	4.944(-30)	7.570(-07)	6.171(-03)	1.662(-02)
6 3 4 6 2 5 010	3310494.176	0.094	2161.2860	29.4571	1.695(-34)	9.691(-08)	3.693(-03)	1.264(-02)
10 2 8 11 1 11 000	3323228.600	0.086	1327.1176	0.0514	1.821(-21)	3.923(-05)	1.661(-02)	2.824(-02)
7 4 4 7 3 5 000	3329185.202	0.013	816.6942	12.3673	1.713(-13)	1.545(-03)	4.168(-02)	4.616(-02)
3 2 2 2 1 1 000	3331458.390	0.012	95.1759	5.6980	3.200(-02)	2.775(-01)	1.527(-01)	9.229(-02)
12 6 7 11 7 4 000	3354519.723	0.137	2321.9057	9.1761	5.252(-37)	3.078(-08)	2.800(-03)	1.097(-02)
9 2 7 10 1 10 010	3395402.766	0.194	2705.1396	0.2152	5.420(-43)	1.969(-09)	1.421(-03)	7.686(-03)
13 7 7 12 8 4 000	3404037.769	0.270	2813.5287	3.0796	1.099(-44)	9.045(-10)	1.172(-03)	6.944(-03)
13 7 6 12 8 5 000	3430497.381	0.328	2813.5122	9.2526	1.100(-44)	9.092(-10)	1.180(-03)	6.995(-03)
14 4 11 15 1 14 000	3440256.583	0.384	2631.2689	0.4321	7.734(-42)	3.379(-09)	1.642(-03)	8.354(-03)

Table 4—Continued

Transition	ν_{ab}(MHz)	Unc.	E_l(cm^{-1})	$\mu^2 S$	I(50 K)	I(200 K)	I(800 K)	I(1500 K)
12 6 6 11 7 5 000	3468263.974	0.172	2321.8131	3.0860	5.282(-37)	3.147(-08)	2.886(-03)	1.133(-02)
11 7 5 12 4 8 000	3482398.878	0.144	2205.6527	0.0386	3.448(-35)	7.277(-08)	3.569(-03)	1.271(-02)
6 4 2 6 3 3 010	3494856.587	0.085	2282.5896	9.8130	2.166(-36)	4.194(-08)	3.118(-03)	1.185(-02)
8 4 5 8 3 6 000	3495358.205	0.016	1006.1159	43.1577	1.889(-16)	4.081(-04)	3.097(-02)	4.031(-02)
14 4 11 13 5 8 000	3498248.829	0.281	2629.3345	5.4299	8.300(-42)	3.464(-09)	1.673(-03)	8.502(-03)
9 5 4 9 4 5 000	3509431.283	0.020	1360.2353	51.8201	5.553(-22)	3.202(-05)	1.644(-02)	2.881(-02)
8 3 6 9 0 9 010	3534844.077	0.146	2512.2828	0.2040	5.596(-40)	8.093(-09)	2.084(-03)	9.607(-03)
7 1 6 7 0 7 000	3536666.711	0.014	586.2435	18.5700	6.850(-10)	8.430(-03)	6.661(-02)	6.097(-02)
14 6 8 14 5 9 000	3538892.918	0.332	2983.3963	32.9237	2.446(-47)	2.732(-10)	8.941(-04)	6.121(-03)
11 4 8 10 5 5 000	3547271.514	0.074	1724.7054	2.9745	1.125(-27)	2.343(-06)	8.619(-03)	2.052(-02)
6 2 5 6 1 6 010	3553520.985	0.106	2042.7533	18.2870	1.210(-32)	2.380(-07)	4.872(-03)	1.515(-02)
6 0 6 5 1 5 010	3566075.414	0.075	1922.8290	16.0025	9.043(-31)	5.652(-07)	6.064(-03)	1.705(-02)
10 3 8 11 0 11 000	3568076.852	0.086	1327.1100	0.1497	1.830(-21)	4.107(-05)	1.771(-02)	3.021(-02)
13 4 9 13 3 10 000	3569620.105	0.156	2414.7234	80.0370	1.871(-38)	1.643(-08)	2.506(-03)	1.065(-02)
6 0 6 5 1 5 000	3599641.679	0.010	326.6255	16.8349	7.794(-06)	5.518(-02)	1.079(-01)	7.953(-02)
3 2 2 2 1 1 010	3601635.514	0.097	1693.6499	5.5060	3.441(-27)	2.957(-06)	9.239(-03)	2.144(-02)
8 3 6 8 2 7 000	3612970.788	0.016	885.6002	34.8092	1.445(-14)	9.917(-04)	3.963(-02)	4.668(-02)
7 2 5 6 3 4 010	3623900.400	0.125	2271.7122	13.3818	3.211(-36)	4.640(-08)	3.285(-03)	1.239(-02)
5 4 1 5 3 2 010	3638527.781	0.065	2130.4943	20.1899	5.161(-34)	1.285(-07)	4.250(-03)	1.424(-02)
7 3 5 7 2 6 010	3639916.806	0.114	2318.5399	10.9426	5.960(-37)	3.322(-08)	3.032(-03)	1.189(-02)
6 1 6 5 0 5 000	3654603.510	0.011	325.3479	50.7123	8.168(-06)	5.622(-02)	1.097(-01)	8.077(-02)
6 1 6 5 0 5 010	3657072.544	0.089	1920.7665	48.3241	9.754(-31)	5.828(-07)	6.226(-03)	1.750(-02)
6 1 5 5 2 4 010	3660797.270	0.121	2024.1526	8.0879	2.367(-32)	2.772(-07)	5.174(-03)	1.586(-02)
8 3 5 7 4 4 000	3669872.287	0.016	927.7439	3.2017	3.176(-15)	7.395(-04)	3.725(-02)	4.550(-02)
11 3 8 11 2 9 000	3674227.170	0.064	1690.6644	57.1298	3.836(-27)	3.060(-06)	9.456(-03)	2.191(-02)
9 2 7 9 1 8 000	3682708.059	0.024	1079.0796	37.0826	1.373(-17)	2.495(-04)	2.847(-02)	3.948(-02)
7 2 6 7 1 7 000	3691315.397	0.013	586.4792	6.1064	6.809(-10)	8.645(-03)	6.918(-02)	6.347(-02)
4 4 0 4 3 1 010	3708481.568	0.049	2005.9170	3.5876	4.564(-32)	3.186(-07)	5.409(-03)	1.634(-02)
11 5 6 10 6 5 000	3718095.717	0.075	1874.9730	9.5087	5.069(-30)	8.185(-07)	6.861(-03)	1.857(-02)
8 5 3 8 4 4 000	3721502.738	0.015	1131.7756	13.7798	2.065(-18)	1.719(-04)	2.614(-02)	3.791(-02)
9 4 6 9 3 7 000	3737021.502	0.022	1216.2312	15.8717	9.900(-20)	9.387(-05)	2.254(-02)	3.510(-02)
4 4 1 4 3 2 010	3740915.716	0.059	2004.8157	10.7218	4.750(-32)	3.229(-07)	5.462(-03)	1.649(-02)
5 4 2 5 3 3 010	3756027.136	0.061	2126.4077	6.6282	5.989(-34)	1.350(-07)	4.405(-03)	1.473(-02)
13 4 10 12 5 7 000	3762739.966	0.182	2300.6850	2.3461	1.135(-36)	3.856(-08)	3.225(-03)	1.248(-02)
12 4 9 11 5 6 000	3776068.455	0.118	1998.9953	8.4162	5.859(-32)	3.386(-07)	5.565(-03)	1.673(-02)
6 4 3 6 3 4 010	3797448.282	0.074	2271.7122	28.1137	3.219(-36)	4.777(-08)	3.425(-03)	1.295(-02)
6 1 5 5 2 4 000	3798281.643	0.012	416.2087	9.1300	3.116(-07)	2.995(-02)	9.639(-02)	7.677(-02)
4 2 3 3 1 2 000	3807258.625	0.013	173.3658	20.2156	1.937(-03)	1.721(-01)	1.495(-01)	9.712(-02)
13 6 7 13 5 8 000	3809788.310	0.222	2629.3345	84.1528	8.340(-42)	3.653(-09)	1.805(-03)	9.215(-03)
15 3 12 16 2 15 000	3830892.705	0.570	2952.3938	0.4183	7.491(-47)	3.588(-10)	1.015(-03)	6.794(-03)

Table 4—Continued

Transition	ν_{ab}(MHz)	Unc.	E_l(cm^{-1})	$\mu^2 S$	I(50 K)	I(200 K)	I(800 K)	I(1500 K)
7 5 3 8 2 6 010	3844194.052	0.149	2595.8129	0.0280	2.786(-41)	4.675(-09)	1.933(-03)	9.596(-03)
7 5 2 7 4 3 000	3855281.345	0.014	931.2371	31.6994	2.808(-15)	7.434(-04)	3.868(-02)	4.750(-02)
8 6 3 9 3 6 000	3858098.971	0.022	1282.9191	0.0412	9.006(-21)	5.924(-05)	2.056(-02)	3.392(-02)
4 4 1 5 1 4 010	3859413.515	0.129	2000.8630	0.0142	5.484(-32)	3.386(-07)	5.656(-03)	1.704(-02)
7 1 6 7 0 7 010	3869939.054	0.122	2180.6429	19.1236	8.526(-35)	9.304(-08)	4.103(-03)	1.438(-02)
7 4 4 7 3 5 010	3883916.369	0.090	2439.9544	11.8138	7.585(-39)	1.444(-08)	2.582(-03)	1.125(-02)
9 2 7 9 1 8 010	3906841.074	0.166	2688.0799	38.6372	1.009(-42)	2.431(-09)	1.661(-03)	8.918(-03)
6 5 1 6 4 2 000	3922858.086	0.014	757.7802	7.3413	1.440(-12)	2.616(-03)	5.367(-02)	5.702(-02)
12 5 8 11 6 5 000	3937072.760	0.127	2144.0463	11.0204	3.182(-34)	1.223(-07)	4.450(-03)	1.514(-02)
15 4 12 16 1 15 000	3941628.787	0.619	2952.3866	0.1381	7.503(-47)	3.650(-10)	1.041(-03)	6.979(-03)
5 5 0 5 4 1 000	3949319.439	0.017	610.3412	11.7074	2.895(-10)	7.588(-03)	7.038(-02)	6.610(-02)
6 5 2 6 4 3 000	3953481.889	0.015	756.7248	21.9621	1.496(-12)	2.649(-03)	5.414(-02)	5.750(-02)
7 5 3 7 4 4 000	3954345.156	0.013	927.7439	10.4622	3.187(-15)	7.741(-04)	3.981(-02)	4.881(-02)
5 5 1 5 4 2 000	3956019.087	0.016	610.1144	3.9005	2.919(-10)	7.608(-03)	7.052(-02)	6.622(-02)
8 5 4 8 4 5 000	3970997.233	0.015	1122.7085	40.1678	2.870(-18)	1.909(-04)	2.814(-02)	4.064(-02)
3 2 1 2 1 2 000	3977046.138	0.011	79.4964	9.4637	5.681(-02)	3.471(-01)	1.840(-01)	1.107(-01)
11 2 9 12 1 12 000	3981742.623	0.133	1557.8478	0.1407	4.574(-25)	8.355(-06)	1.290(-02)	2.684(-02)

Table 5. The Rotational Partition Function of Water Vapor

Temperature	Q_{rs}	Correction
9.375	1.2572	1.00000000
18.750	3.0332	1.00000000
37.500	8.5802	1.00000000
50.000	12.9613	1.00000000
75.000	23.1702	1.00000000
100.000	35.1523	1.00000000
150.000	63.6774	1.00000000
200.000	97.4129	1.00000000
225.000	116.0195	1.00000000
300.000	178.1163	1.00000031
400.000	274.5588	1.00001526
500.000	386.2616	1.00016408
800.000	818.9779	1.00640974
1000.000	1193.9312	1.02295710
1500.000	2429.2597	1.14104678

Figure 1. A schematic outline of the LTG-GaAs THz photomixer spectrometer. In this three laser system, lasers #1 and 2 are locked to different longitudinal modes of a single ultralow thermal expansion coefficient reference cavity, and laser #3 is phase locked to laser #2 with a tunable microwave source. Lasers #1 and 3 are used to form the tunable THz beat note.

Figure 2. Predicted LTE spectra of water vapor from 0.5 - 4 THz for rotational temperatures of 50, 200, 800, and 1500 K. The column density is the same for all four plots. While the intensity is arbitrary the scaling factor is the same for all four plots, and so the relative intensities are meaningful.

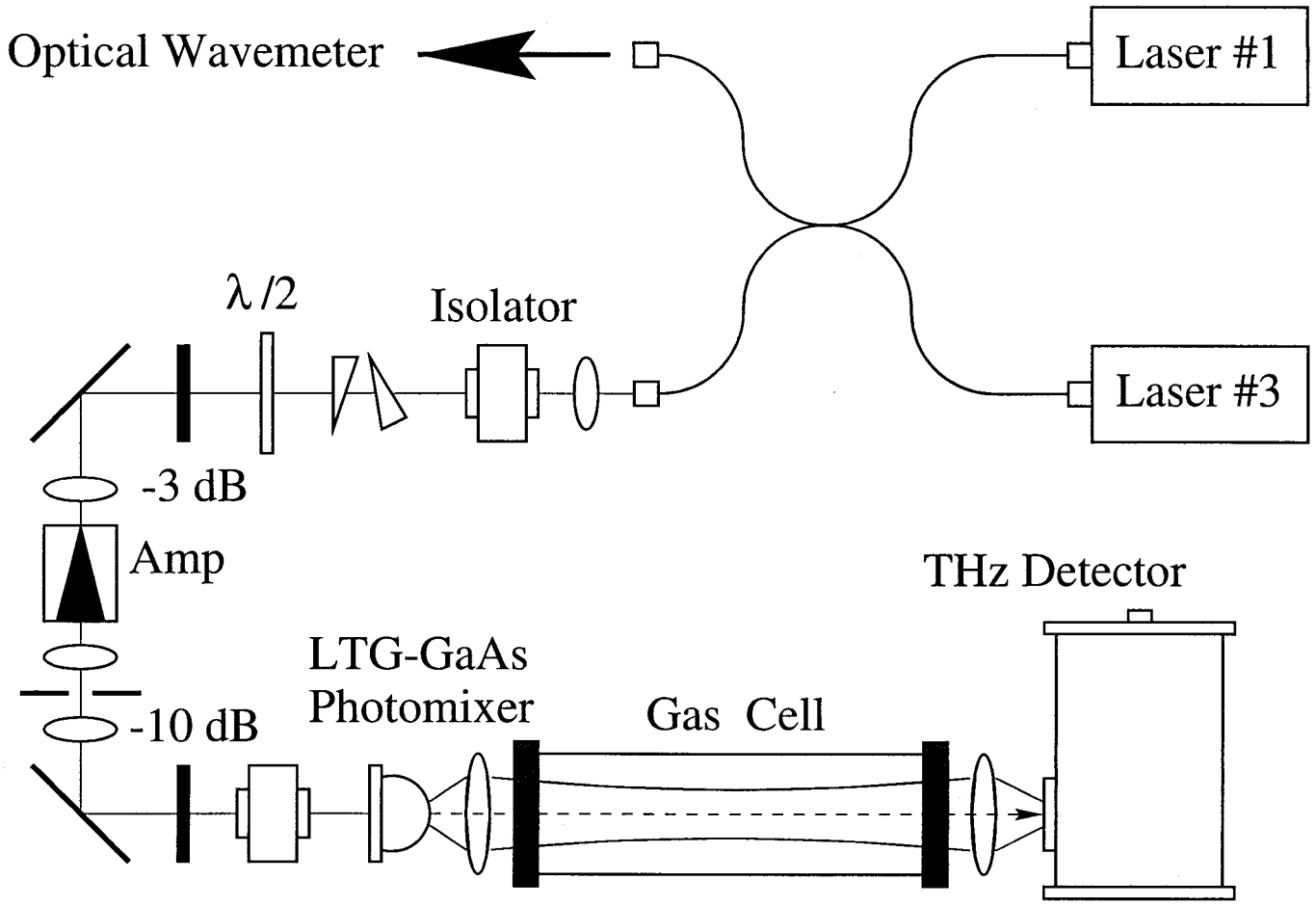
Optical Wavemeter
Laser #1
Laser #3
λ/2
Isolator
-3 dB
Amp
-10 dB
LTG-GaAs
Photomixer
Gas Cell
THz Detector

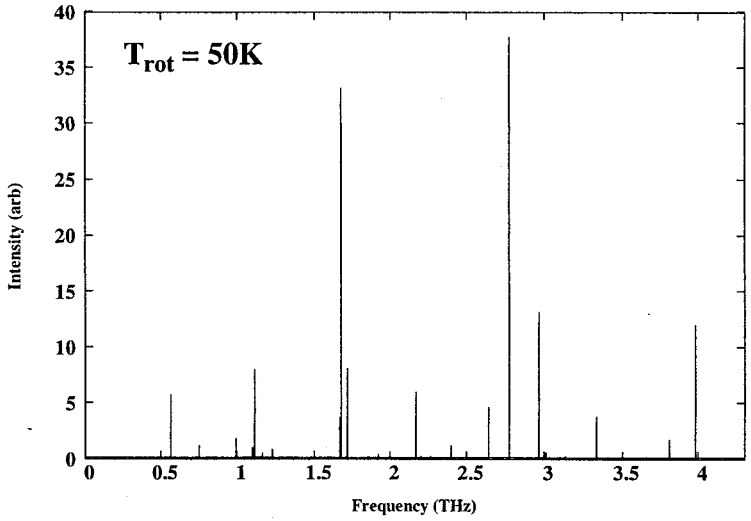
T_{rot} = 50K
Intensity (arb)
Frequency (THz)
0
5
10
15
20
25
30
35
40
0.5
1
1.5
2
2.5
3
3.5
4

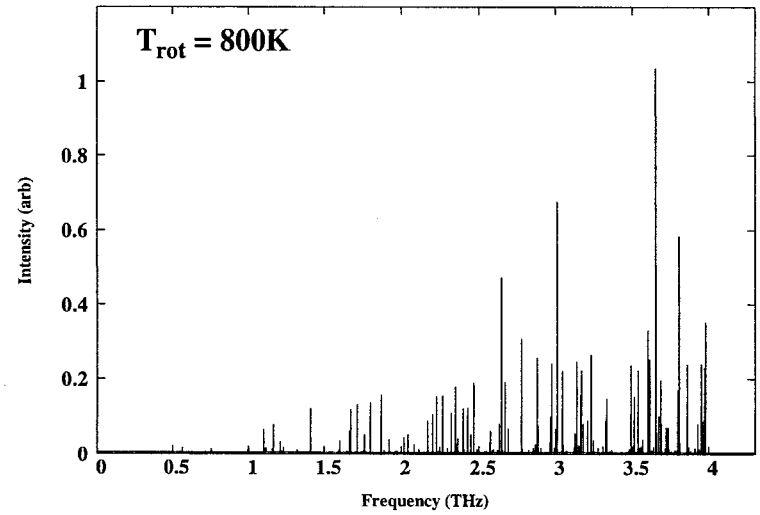
T_{rot} = 800K
Intensity (arb)
Frequency (THz)
0
0.2
0.4
0.6
0.8
1
0.5
1.5
2
2.5
3
3.5
4

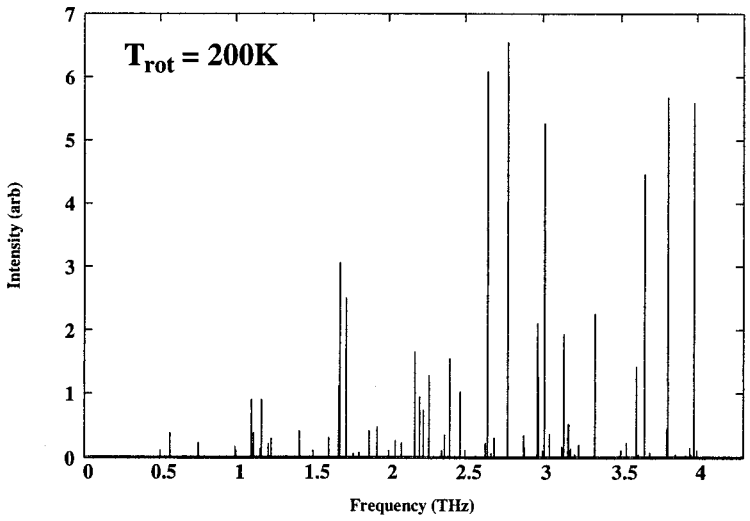
T_{rot} = 200K
Intensity (arb)
Frequency (THz)
0
1
2
3
4
5
6
7
0.5
1
1.5
2
2.5
3
3.5
4

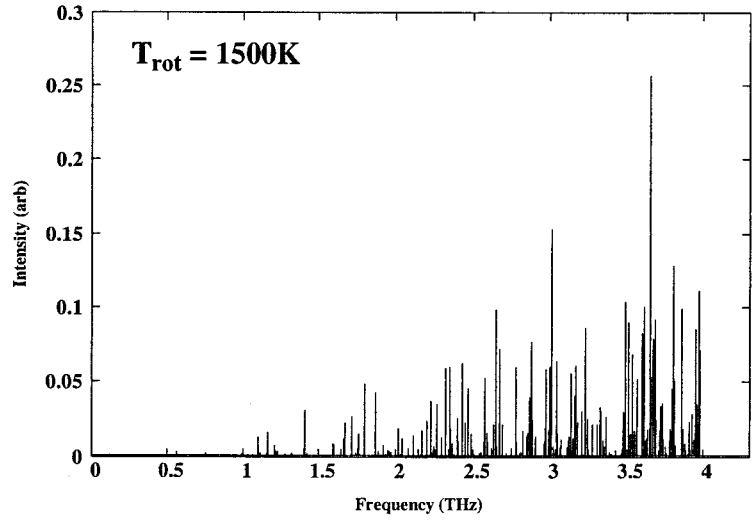
T_{rot} = 1500K
Intensity (arb)
Frequency (THz)
0
0.05
0.1
0.15
0.2
0.25
0.3
0.5
1
1.5
2
2.5
3
3.5
4